Reply to Referee #1 (Simon Horton)

We thank Simon Horton for the positive and very constructive feedback. In the following we will reply to the comments point-by-point. Your comments are in blue, replies in black.

General comments:

This paper investigates how stability indices predicted by snowpack models are impacted by uncertainties in the weather inputs. Spatial snowpack simulations could be valuable for avalanche forecasting, however there are numerous challenges in producing accurate spatially distributed weather inputs for these models. This paper provides a strong quantitative analysis of what the implication of these uncertainties are when assessing snowpack stability. The sensitivity analysis uses weather data for a situation where a prominent weak layer formed in the snowpack and subsequently resulted in avalanche activity throughout the season. Although only a single scenario is investigated, the implications of various biases added into the data provides a robust analysis of how uncertainties in different weather inputs impacts weak layer formation, slab properties, and snowpack stability. The paper provides a significant contribution by improving the interpreting stability indices and illustrating the need for improved prediction of snowfall patterns. The methods are valid and rigorous, and the manuscript is well structured, organized, and easy to follow. My comments are relatively minor and could improve the manuscript by clarifying a few details and expanding on some interesting results.

Specific comments:

An interesting result that could use more discussion is explaining why the uncertainties resulted in unequal proportions of properties relative to the reference run. For example, Fig. 3 shows the majority cases had weak layers with lower densities and larger grain sizes than the reference run, and Fig. 9 shows the majority of cases had smaller critical crack lengths than the reference run. While such trends are reported throughout the results, they are not explained in the Discussion. Do these results mean (a) the distribution of input uncertainties were biases towards these results, (b) there

were interaction effects between different combinations of biases that favoured these results, (c) some type of non-linearities in the model, (d) something else? If related to the biases, which biases resulted in these trends and why?

The results shown in Figure 3 resulted from the lognormal bias distribution in P, resulting in more runs with lower precipitation than the reference run (see Fig 1 below). We addressed this in the Discussion section (p.16, l.300-303): "Introducing a lognormal distribution for the bias in precipitation resulted in unequal proportions relative to the reference run (e.g. Figures **??** and **??**). A coefficient of variation for the lognormal distribution was chosen as this reflects typical snow depth patterns observed in mountainous terrain (e.g. Liston, 2004). Hence, relatively more simulations had smaller P values than the reference run." Furthermore, we added in p.17,l.348-350: "As thinner snow covers generally have a lower density (less settlement) and experience larger temperature gradients, weak layer density decreased and grain size increased with decreasing precipitation (Figure 3b and c)."

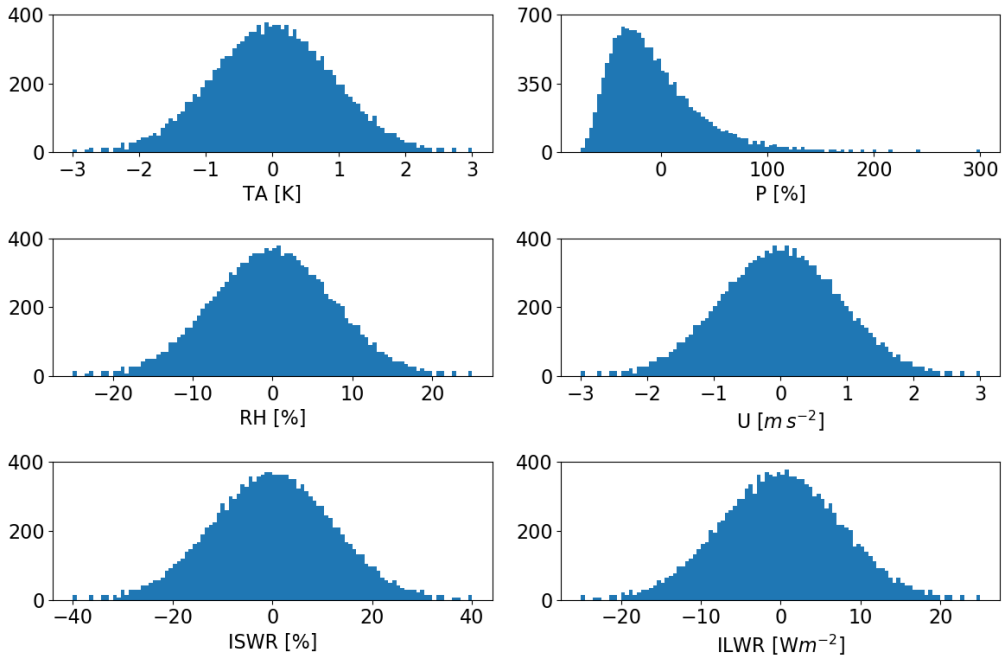

Figure 1: Distribution of meteorological input uncertainties.

There could be a bit more clarity on how the biases were applied to the weather data, since the distribution of weather inputs has a substantial effect on the results. I interpreted the method as follows: for a given time series, a bias b was randomly chosen for each variable and then that single value applied to the variable for the entire season. This could be stated more explicitly. If random biases were selected for each variable you would expect a roughly equal proportions of different bias combinations (e.g. samples with P+/TA+, P+/TA-, P-/TA+, P-/TA-). Would such combinations reflect the distribution of conditions you would actually expect to find in nature? Is this method consistent with other sensitivity studies using weather data? I suspect the method of applying these biases resulted in the skewed proportions discussed in the previous comment.

Indeed, your interpretation of how we applied the biases is correct. We mentioned this more explicitly in the revised manuscript (p.6, l.148). Biases were applied randomly to each variably and independently of other variables. As such, we did not account for correlations between variables typically observed in nature. Nevertheless, the Sobol' method is advantageous in that it is model independent, can handle non-linear systems, and is among the most robust sensitivity methods (Saltelli and Annoni, 2010; Saltelli, 1999). The skewed proportion from the previous comment likely come from the lognormal distribution of bias introduced for P (see answer above) and not from the combination of different biases.

A limitation of the study is that it considers a single type of weak layer and snowpack structure combinations (i.e. early season facets above a crust). The type of weak layer considered in this study is important and should be stated in more places (e.g. abstract and conclusions). While briefly discussed in lines 317-323, many of the results likely still generalize to more types of snowpack conditions (especially the slab properties). For surface hoar, a major sensitivity is the exposure time of the layer on the surface in between precipitation events. A light amount of snow could stop surface hoar growth in a much more dramatic way than facets. This again strengthens the argument that precipitation patterns (spatial, quantity, and timing!) are critical. While the details of surface hoar formation are outside the scope of this study, acknowledgement of this limitation and more discussion of what results likely transfer to other weak layers would be valuable.

Thanks for the suggestion. We mentioned the type of weak layer explicitly in the Abstract (p.1, l.8): "Simulations were performed for a winter season, which was marked by a prolonged dry period at the beginning of the season. During this period, the snow surface layers transformed into faceted and depth hoar crystals, which were subsequently buried by snow. The early season snow surface was likely the weak layer of many avalanches later in the season." We will also mention the type of WL explicitly in the Conclusions: "We investigated the sensitivity of two modeled snow instability metrics for a weak layer consisting of faceted and depth hoar crystals..." We agree that our results for the slab properties are indeed more transferable to other types of weak layers. However, since we already discussed this in lines 336-342, we do not feel that this needs to be pointed out more prominently.

While the paper touches on most of the interesting results, there are a few minor results listed in the Technical comments that could also be discussed (e.g. why does wind speed impact shear strength?, why does weak layer grain size on 2 Jan not show sensitivity to temperature or radiation as might be expected for facets?)

We added more discussion as suggested in p.167,l.339-355 in the revised manuscript (see answers below to technical comments).

The discussion section could be reduced as there is substantial repetition from previous sections (e.g. lines 281-282 repeat the methods, lines 301-306 repeat introduction/motivation of study, lines 307-309 repeat methods, etc.). While this section is well written and examines interesting results, the repetition of why and how the study was done is unnecessary.

We removed redundant passages in the Discussion section as suggested.

The conclusions could have greater a emphasis on the contributions of the study. Although well written, they primarily focus is summarizing the results.

We agree and put more emphasis on the contributions (p.19, l. 4066-409 and l. 415-416).

Overall the figures are clear, legible, and are effective at communicating the key results of the study.

Technical comments:

p1 l8: It would be helpful for the abstract to briefly explain the snowpack conditions for the case study (especially the fact the type of weak layer was early season facets above a crust).

We mentioned the snowpack conditions in the Abstract as suggested (p.1, l.7-9), by adding: "Simulations were performed for a winter season, which was marked by a prolonged dry period at the beginning of the season. During this period, the snow surface layers transformed into faceted and depth hoar crystals, which were subsequently buried by snow. The early season snow surface was likely the weak layer of many avalanches later in the season."

p1 l 17: add "(more stable)" following crack length sentence for consistent structure.

We changed as suggested.

p1 l15 "sensitive to precipitation"

We changed as suggested.

p2 l49-52: It would be helpful to explicitly explain how to interpret SK38 and rc in relation to initiation and propagation (e.g. "low values of SK38 indicate initiation more likely, low values of rc indicate propagation more likely")

Thanks for suggestion. We explained the instability metrics in more detail in the revised manuscript (p.2,l.52).

p2-3 l 53-74: I appreciate how this paragraph concludes by identifying the clear gap in literature that this study addresses, however most of the paragraph reads like a long list of studies and the link to your research question isn't always apparent. I think by rewording some sentences it could be clearer how these studies relate to your research question. Also, Andrew Slaughter's PhD thesis (Slaughter, 2010) performs a SOBOL sensitivity analysis for formation of several types of weak layers and is relevant to this study.

As suggested, we rewrote this section (p.2, l.53 - p.3, l.69) to make it more focused. Thanks for pointing out the work by Slaughter, which is indeed relevant to this study.

p4 l1: Just a comment: the weekly snow profiles aren't directly used in your study, although I assume they were important for understanding the avalanche conditions that you describe.

We added the weekly snow profiles to Figure 1 to facilitate validation of the model runs as suggested by referee 2.

p4 l115: Thickness-weighted averaging may smooth out the properties of the most unstable layer(s) that may contain the critical properties for avalanche release. Could this averaging method somehow impact the biases favouring the formation of more unstable layers?

We agree that using thickness-weighted averaging may smooth out properties of the most unstable layers. However, since there is no unambiguous definitions of the most unstable layer, as layers with a lowest rc value do not necessarily have the lowest SK38 value, we decided to focus on average properties. Note that initially we also tried to focus on single layers, rather than average properties, and the overall observed trends were very similar. We do not believe, that averaging layer properties favours more unstable layers (see answer to first comment above).

p4 l116: "shear strength of the weak layer. . ."

We changed as suggested.

p4 l116: I understand you present the SK38 and rc derivations in general form, but would it make sense to use the bar notation for the variables that you substitute with thickness-weighted averages (such as slab and weak layer densities)?

Thanks for noting this unclear explanation in the text. The instability metrics were calculated for each layer, as presented in the manuscript, and then thickness-weighted average instability metrics were reported. We clarified this in the manuscript, by using the bar notation more consistently through-

out the manuscript as suggested and adding (p.6, l. 142): "SK38 an r_c were calculated for each of the weak layers as defined above and thickness-weighted mean instability metrics $\overline{SK38}$ and $\overline{r_c}$ were determined from all weak layers"

p5 l131-134: Please provide a written explanation of what this correction factor accounts for.

We introduced the correction factor providing the following explanation (p.6, l.137): "Richter et al. (2019) introduced the correction factor Fwl to replace two variables of the original parameterization (Gaume et al., 2017), which were not well defined in SNOWPACK. The factor Fwl accounts for weak layer density and grain size and considerably improved the rc parameterization, and it ensures that layers with larger grains have lower rc values (Richter et al., 2019)."

p5 l 136: In the abstract you specify the uncertainty values are typical for extents of 2 km and elevation changes of 200 m. It would be worth including that somewhere in the text.

We included the interpretation of uncertainties at the end of this paragraph (p.6, l.155): "With the given ranges and distributions (Table 1), biases can be interpreted as differences typically observed within a spatial distance of around 2 km and an elevation range of around 200 m. For example, around 68 % of the simulations have a bias in air temperature of -1 K to +1 K, which cover temperature differences within an elevation band of around 200 m. Uncertainties in P will yield rather shallow or rather thick snowpacks as typically observed for wind exposed or wind sheltered slopes."

p6 l150: Please specify here whether Case ALL has a unique set of biases or simply concatenates the two other cases.

We stated that for each scenario (case WL, case SL, and case ALL) a unique set of biases was introduced (p.7, l. 167).

Sect. 2.4: This section could use some additional explanation. First, it would be helpful to move the written description of what ST_i means (line 160-161) before the mathematical definition in Eq. 5. On line 162 you describe a 'perfect additive model', but do not explain whether this is important or how

that idea applies to this study. It's not clear what information is contained in the A and B matrices as you simply describe their dimensions rather than their content, and thus the importance of AB is unclear. Without explanation I'm wondering if B is a matrix full of biases b you introduce in Table 1 (i.e. the same letter).

We improved the clarity of the explanation in this section. First, we moved lines 160-162 above equation (5) and removed the reference to a perfect additive model, as it does not apply to our case (p.7, l.173): "In a global sensitivity analysis, the total-order sensitivity index STi describes the variance in output variables Y, i.e. snow properties, due to uncertainties introduced to a specific meteorological input Xi, while including interactions with other forcing errors. Values for STi range from 0 (no sensitivity) to 1 (one-to-one sensitivity)." We also better explained the content of the matrices A and B, by adding this sentence (p.7., l.179): "The elements of the two independent matrices A and B thus consist of biases for the input variables randomly picked from the ranges and distributions shown in Table 1."

Sect. 3.1: This section provides a very clear and helpful practical explanation of the case study.

Thank you very much for this feedback.

p8 l195: A more intuitive wording would be something like "We present weak layer and slab properties on 2 January with results from the reference run and case WL because..."

We changed as suggested.

p8 l197: In the methods your weak layer group consists of more than just facets (e.g depth hoar and surface hoar), does the "percent facets" variable actually mean percent of weak layers or literally percent facets and there was no depth hoar or surface hoar?

Indeed, this variable was unclear and we defined it more clearly in the Methods section (p.5, l.112): "Hence, weak layer thickness D_{wl} was defined as the thickness of all layers consisting of either facets, depth hoar or surface hoar, which were deposited between these two dates. The percentage of facets (%

facets), was defined as D_{wl}, divided by the total thickness of all layers which were deposited between these two dates (see Section 3.2.1)."

Fig. 3 and 4: Would a more logical progression be showing Fig. 4 first to show which input uncertainties had the greatest effect then show Fig. 3 to show the direction of the effect? Seeing which weather input had the greatest impact on a given property would help explain why a specific scatter plot is being shown. Same logic applies to Fig. 5 and 6 and 9 and 10. Just a thought.

We changed the order of the Figures and the corresponding text as suggested.

p9 l204: Is weak layer thickness also calculated as an average of each individual layer, or was it the sum of all identified weak layers? The sum seems more meaningful.

The weak layer thickness was calculated as the sum of all identified weak layers. Thanks for noting this unclear definition. We will clarify this by adding (p.5, l.112): "Hence, weak layer thickness D_{wl} was defined as the thickness of all layers consisting of either facets, depth hoar or surface hoar, which were deposited between these two dates."

p9 l204-205: This result about the impact of precipitation is somewhat unique to how this weak layer is being identified (as all layers forming over a date range), and it is not necessarily intuitive to think about how precipitation during a formation period impacts weak layer formation. It would be helpful to reiterate what precipitation means for this specific case. Also, wouldn't you expect grain size to be more sensitive to air temperature (and perhaps the radiation variables) given the weak layers were faceted crystals?

We agree that repeating the meaning of precipitation would be helpful for interpretation, so we mentioned this in the text (p.10, l.233): "Increasing P led to denser weak layers and smaller grains (Figure 4b,c). Positive biases in P result in thicker snowpacks, as would typically be observed in wind-sheltered locations." Regarding the sensitivity of weak layer grain size to air temperature and radiation, this result is indeed somewhat surprising, since both these parameters are highly relevant for the energy input at the snow surface and thus snow surface temperature and temperature gradients across

the snowpack. However, in December, the energy balance at the snow surface is generally negative (i.e. surface cooling), as days are very short and incoming short-wave radiation is very low. Even with positive air temperature, the snow surface often stays well below zero, except on very steep south-facing slopes (higher incoming short-wave radiation), or when there is a thick cloud cover (higher incoming long-wave radiation). Since there was generally only limited cloud cover in December 2016 (low incoming long-wave radiation), and the simulations were performed for a flat field site (low incoming short-wave radiation), we believe our results are plausible. We discussed this in more detail in p.17, l.340-348 in the revised manuscript.

p9 l208: It would be interesting to discuss why weak layer shear strength was most sensitive to wind speed as well as the direction of the relationship (i.e. did increasing wind typically result in higher or lower shear strength?). This result is not necessarily the most intuitive and could be discussed more.

The weak layer consisted of layers deposited between two given dates and consisting of persistent grain types (i.e. DH, FC or SH). Shear strength in SNOWPACK is a function of grain type and density. As new snow density in SNOWPACK depends on wind velocity, we believe that shear strength depended on wind velocity for the case WL. We discussed this in more detail in p.17, l.350 in the revised manuscript.

p11 l211: It would be helpful to introduce this date the same way as 2 Jan by introducing the fact you now consider all three cases before you start reporting results.

We introduced the date as suggested: "According to Section 3.2.1, we present weak layer and slab properties on 9 March 2017 by considering all three cases with results from the reference run."

Fig. 5: The load-P subplots present obvious results and it's not clear there's added value in graphing these relationships.

We agree that the subplots for the load are rather trivial. Nevertheless, we intentionally added these figures to highlight that although load was most sensitive to precipitation in all three scenarios, for case WL the variability in slab load was almost imperceptible.

p12 l223: High slab load than what? The reference case?

That is correct. We added that slab load was higher than in the reference run.

p12 l227: Does it make sense that ST would change between 2 Jan and 9 mar if Case WL uses the reference data from 2 Jan onwards?

You are correct to assume that ST does not change much between 2 January and 9 March. Nevertheless, there are some subtle changes, as different weak layers on 2 January do not necessarily react exactly the same to the same slab. Indeed, harder and denser weak layers will settle less than soft low density weak layers. As such, there are some changes in ST between 2 January and 9 March. We discussed this in p.18, l.353.

p12 l233-243: This paragraph is very well written and easy to follow!

Thanks.

Fig. 8: Is it correct to follow the points as a time series starting from the bottom left? If so, including a line connecting the points (and perhaps even an arrow) could make it clearer this shows evolving stability properties rather than an independent scatter of data points.

Indeed, this is the case. We improved as suggested.

p13 l 254: Could you provide a similar summary for rc as done for SK38 in line 247 ("This suggests, that different slabs influenced SK38 more than different weak layers"). It appears from Fig. 9 rc was equally impacted by weak layer and slab properties.

We agree with your interpretation and provided this summary (p.15, l.282): "This suggests that rc was equally impacted by weak layer and slab properties."

p14 l259-268: I found this paragraph slightly confusing to read. Perhaps some parts could be reworded or even some of the interpretation moved to the Discussion.

We improved the paragraph as suggested.

p18 l320-324: This result agrees with Horton et al. (2015) who examine how variability in meteorological fields from NWP models across elevations resulted in reasonable predictions of surface hoar formation. Slaughter (2010) also analyzes sensitives of surface hoar and other weak layers to weather inputs.

Thanks for this input, we referd to these studies in the revised manuscript (p.17, l.333-338): "This result agrees with Horton et al. (2015) who examined how variability in meteorological fields from numerical weather prediction models across elevations resulted in reasonable predictions of surface hoar formation. However, we only looked at one type of weak layer. The formation and subsequent burial of surface hoar might be more sensitive to other meteorological parameters, such as wind speed (Stössel et al., 2009). In fact, Slaughter (2010) investigated the sensitivity of near-surface faceting and surface hoar formation at mid-day and mid-night to input parameters using a snow thermal model. He found incoming long-wave radiation to be the most dominant input parameter, although they did not investigate the sensitivity to precipitation."

p18 l340-342: This is a very practical take away from this study that supports practical forecasting experience, and could be a valuable application of snowpack models.

Thanks. As suggested above, we added this as an application to the Conclusions.

p18 l343: "than in weak layer shear strength"

We changed as suggested.

p18 l344-345: These results could be supported by citing field studies that describe the lag in weak layer shear strength increases after loading, such as Jamieson et al. (2007) who also give interesting implications on spatial variability of stability indexes due to variable precipitation.

We do not entirely agree that field observations of the lag in shear strength

increase after loading support our results. In our case, we are discussing observed trends in SK38 in March, after several precipitation events and when the weak layers are already more than 60 days old. We clarified this in p.18, l.374-379, by adding that during periods without precipitation, SK38 slightly increased due to the lagged increase in shear strength (Jamieson et al., 2007). Whereas, the overall decrease in SK38 (i.e. low values end of March) was explained by a stronger increase in slab load than in weak layer shear strength between January and March (i.e. shear strength remained low in March). The same effect resulted in a decrease in the stability index (e.g. SK38) with increasing P on 9 March 2017 (Figure 9c), i.e. slab load increased stronger than weak layer shear strength with increasing P.

p18 l351: How do you explain this counter intuitive result where SK38 remain slow into spring? It would seem that since the load continues to increase that the weak layer strength must have remained low. Was this the case?

After 10 March 2017, the slab load hardly increased, since there was almost no precipitation (see Figure 1). During the period of slab formation, the slab load increased considerably stronger than the weak layer shear strength, resulting in low values of SK38 in spring (see answer above). This is a well-known problem with SK38, and why it should not be used for weak layers that are buried deeper than about 100 cm (Schweizer et al., 2016).

p19 l360-361: How does this sentence about precipitation tie back to the theme of climate change?

We added in p.19, l.395: "With climate change, extreme events may become more frequent, e.g. prolonged dry periods - favoring the formation of weak layers - may alternate with more extreme precipitation events (CH2018, 2018) - with partly opposing effects on our snow instability metrics."

Reply to Referee #2

We thank the referee for the positive and very constructive feedback. In the following we will reply point-by-point. Your comments are in blue, replies in black.

In their manuscript "Sensitivity of modeled snow stability data to meteorological input uncertainty", the authors perform a sensitivity analysis of modeled snow stability data and indices to uncertainties in the meteorological forcing data. For this purpose, the widely used snow cover model SNOWPACK is forced with disturbed meteorological input data implementing different bias scenarios on the single meteorological parameters resulting in 14,000 simulations.

General comments:

I understand that this is a model sensitivity study and the model has been validated in other studies. However, I would highly appreciate if you could add some model validation for your presented case study to get a better understanding of the model performance especially with respect to the model's sensitivity to forcing errors. As I understand, you have some observed profiles available, maybe directly at the WFJ site? You could add a validation plot in Sect. 2.2 (e.g. accompanying Fig. 1?) for the undisturbed reference run after averaging the SNOWPACK layers as described there. I see that you perform kind of validation by comparing the results to avalanche activity and AAI, but it would be very valuable to have a direct comparison to measurements, in the best case even within the uncertainty range figures (Figs. 3 and 5). In addition, you should add modeled snow depth from the reference run to Fig. 2 (which I assume is observed snow depth, information should be added to the Fig. caption). All this would bring the findings of the impacts of forcing uncertainty on modeled snow stability in better context to reality and build more trust in the models to be used in operational forecasting.

As suggested, we added the observed snow profiles to Figure 1. We then presented weak layer and slab layers with observed snow stratigraphy and the reference run in section 2.2. Furthermore, we added modeled snow depth from the reference run to Figure 2. As we do not have manually observed snow profiles at the dates, we present in this study, we cannot show observed

weak layer properties. Furthermore, this would need considerably more details on how slab and weak layer properties were presented from manual snow profiles (e.g. grain size 1 is defined by average grain size of all crystals and grain size 2 is defined by average grain size of largest crystals), so we prefer not add manual data to Figures 3 and 5.

I think the bias/disturbing procedure to produce the disturbed meteorological forcings within the given ranges needs some more explanation. Specifically: at what time scale are the errors applied? Is it a constant offset applied to the time series for a scenario or does it have some time variability within the scenario? This should then be referred to in L. 301-306.

We explained, how uncertainties are applied to the input in more detail. We explicitly mentioned in p. 6, l.147, that a bias b was randomly chosen for each variable and then that single value applied to the variable for a given time series. Furthermore, we explicitly mentioned, that the given time series ranged from 1 October 2016 to 2 January 2017 for case WL, 3 January 2017 to 1 May 2017 for case SL and the entire season for case ALL.

Specific Comments:

At some points in the manuscript you use "snow height", but mostly "snow depth". Please use "snow depth" consistently.

For more consistency, we changed snow height to snow depth throughout the manuscript as suggested.

L. 15: "...sensitive to precipitation..."

We changed as suggested.

L. 55: You state: "However, only a few studies have so far assessed the uncertainty of snow cover models." I would rather change this to, e.g., "However, only a few studies have so far assessed the impact of forcing uncertainty on the performance of snow cover models." because there are many studies available in literature which assess the performance and uncertainty of snow cover models in general.

We changed as suggested.

L.105: "For the sensitivity analysis, we introduced uncertainties to the meteorological input." This sentence could be removed here, as you explain this in the next sections.

We removed this sentence as suggested.

L. 150: I suggest to remove the sentence "For each scenario, 14,000 simulations were performed." here, as the number of simulations is explained in the following section 2.4. You could instead extend the last sentence of 2.4 (L. 170), e.g. like "...for each of the three applied scenarios."

As suggested, we moved the content of this sentence to the next section (p.8, l.188).

L. 274 "Precipitation influences weak layer and slab properties." instead of "Precipitation influences weak and slab properties."

We changed as suggested.

Sensitivity of modeled snow stability data to meteorological input uncertainty

Bettina Richter[1], Alec van Herwijnen[1], Mathias W. Rotach[2], and Jürg Schweizer[1]

[1]WSL Institute for Snow and Avalanche Research SLF, Davos, Switzerland

[2]Institute for Atmospheric and Cryospheric Sciences, University of Innsbruck, Innsbruck, Austria

Correspondence: Bettina Richter (richter@slf.ch)

Abstract. To perform spatial snow cover simulations for numerical avalanche forecasting, interpolation and downscaling of meteorological data are required, which introduce uncertainties. The repercussions of these uncertainties on modeled snow stability remain mostly unknown. We therefore assessed the contribution of meteorological input uncertainty on modeled snow stability by performing a global sensitivity analysis. We used the numerical snow cover model SNOWPACK to simulate two snow instability metrics, i.e. the skier stability index and the critical crack length, for a field site equipped with an automatic weather station providing the necessary input for the model. ~~Uncertainty ranges for meteorological forcing covered typical differences observed within a distance of 2 km and an elevation change of 200 m~~Simulations were performed for a winter season, which was marked by a prolonged dry period at the beginning of the season. During this period, the snow surface layers transformed into layers of faceted and depth hoar crystals, which were subsequently buried by snow. The early season snow surface was likely the weak layer of many avalanches later in the season. Three different scenarios were investigated to better assess the influence of meteorological forcing on snow stability during a) the weak layer formation period, b) the slab formation period, and c) the weak layer and slab formation period. For each scenario, 14'000 simulations were performed, by introducing quasi-random uncertainties to the meteorological input. Uncertainty ranges for meteorological forcing covered typical differences observed within a distance of 2 km or an elevation change of 200 m. Results showed that a weak layer formed in 99.7% of the simulations, indicating that the weak layer formation was very robust due to the prolonged dry period. For scenario a), modeled grain size of the weak layer was mainly sensitive to precipitation, while the shear strength of the weak layer was sensitive to most input variables, especially air temperature. Once the weak layer existed (case b), precipitation was the most prominent driver for snow stability. The sensitivity analysis highlighted that for all scenarios, the two stability metrics were mostly sensitive to precipitation. Precipitation determined the load of the slab, which in turn influenced weak layer properties. For case b) and c), the two stability metrics showed contradicting behaviors. With increasing precipitation, i.e. deep snowpacks, the skier stability index decreased (less stable). In contrast, the critical crack length increased with increasing precipitation (more stable). With regard to spatial simulations of snow stability, the high sensitivity on precipitation suggests that accurate precipitation patterns are necessary to obtain realistic snow stability patterns.

1 Introduction

Snow avalanches are a natural hazard, which can endanger roads, villages and human lives. A dry-snow slab avalanche starts with failure within a weak layer (Schweizer et al., 2003a). Such weak layers often form close to the snow surface. If subsequently, weak layers are covered by new snow, they can persist the entire season. Whether a failure in a weak layer is prone to propagate, depends on the complex interaction between slab layers and the weak layer (van Herwijnen and Jamieson, 2007). The two key processes in avalanche release, failure initiation and crack propagation, can respectively be described with a stress-strength approach (expressed as stability index) and a fracture mechanical approach (considering the critical crack length as observed in a propagation saw test) (Reuter and Schweizer, 2018; Schweizer et al., 2016).

When assessing the avalanche danger, avalanche forecasters rely on snow instability data, combined with measured and forecasted meteorological data (McClung and Schaerer, 2006). Data on snow instability ~~includes~~ include recent observations of avalanches, or whumpfs and shooting cracks (Jamieson et al., 2009). Such signs of instability are very rare, especially on days with low avalanche activity (Reuter et al., 2015). Information on snow stratigraphy and so-called stability tests then becomes important. Unfortunately, these manual observations are relatively time-consuming point observations and sometimes dangerous to obtain so that the temporal and spatial resolution of snowpack data is limited. Detailed snow cover models, which simulate the full snowpack stratigraphy, can help fill this gap (e.g. Lafaysse et al., 2013; Morin et al., 2020) provided they include information on snow instability (e.g. Schweizer et al., 2006; Lehning et al., 2004; Vernay et al., 2015).

The two most advanced snow cover models are Crocus (Brun et al., 1992; Vionnet et al., 2012) and SNOWPACK (Lehning et al., 2002; Wever et al., 2015). ~~SNOWPACK can be used for one-dimensional simulations or for distributed snow cover modeling, when coupled with the three-dimensional model Alpine3D (Lehning et al., 2006).~~ Crocus is part of the French model chain SAFRAN–SURFEX/ISBA-Crocus–MEPRA (S2M), which predicts the regional avalanche danger (Durand et al., 1999; Lafaysse et al., 2013). The meteorological model SAFRAN provides the input for Crocus, which simulates the stratigraphy on virtual slopes for different elevations and aspects. MEPRA is an expert system, which derives the avalanche danger by combining various stability indices with a set of rules to evaluate the simulated snow stratigraphy in terms of stability classes (Giraud and Navarre, 1995). ~~Recently, Vernay et al. (2015) drove S2M with an ensemble of atmospheric forcings to estimate the uncertainties from numerical weather prediction models. Meteorological input clearly influenced the forecasted avalanche hazard and was assumed to be the main source of uncertainty. How these uncertainties influenced snow stability in more detail was not investigated.~~

The snow cover model SNOWPACK can be used for point simulations or for distributed snow cover modeling, when coupled with the three-dimensional model Alpine3D (Lehning et al., 2006). SNOWPACK is forced with meteorological data from either automatic weather stations (Lehning et al., 1999) or numerical weather prediction models (Bellaire et al., 2011), and snow instability metrics can be derived from simulated stratigraphy (Lehning et al., 2004). The skier stability index ~~SK_{38}~~ SK38 relates to failure initiation and compares the shear strength of a weak layer with the shear stress acting on the weak layer due to the load of the overlaying slab and a skier (Föhn, 1987; Jamieson and Johnston, 1998; Monti et al., 2016). The critical

crack length r_c relates to crack propagation and was implemented into SNOWPACK by Gaume et al. (2017) and refined by Richter et al. (2019). Low values of SK38 indicate that initiation is likely, low values of r_c indicate that propagation is likely.

When modeling spatially distributed snow stratigraphy and snow instability, uncertainties may arise from numerical weather prediction models or due to spatial interpolation of meteorological data. For numerical avalanche forecasting it is of particular importance how sensitive these stability criteria are to meteorological input uncertainty. ~~Uncertainties due to spatial interpolation of meteorological data may arise when modeling distributed snow stability.~~ However, only ~~a few studies have so far assessed the uncertainty of~~ few studies so far addressed the sensitivity of modeled snow instability estimates. Previous snow sensitivity studies typically focused on snow depth or snow water equivalent (SWE). Uncertainties in modeled snow ~~cover models. Côté et al. (2017) investigated the sensitivity of modeled snow height to three different weather models for five different automatic weather stations. They found that differences in forecast precipitation influenced modeled snow height. Bellaire et al. (2011) forced the SNOWPACK with output from a numerical weather prediction model . They showed that the weather prediction model generally overestimated precipitation events above 3 mm and therefore proposed different filtering methods for forecasted precipitation, which influenced modeled snow depths. By applying a constant scaling factor for forecasted precipitation, SNOWPACK could reproduce measured snow depths and critical snow layers. Schlögl et al. (2016) systematically investigated the impact of different model setups on the robustness of modeled snow water equivalent. They forced the distributed model Alpine3D with data from automatic weather stations and showed that the coverage of weather stations can influence modeled snow water equivalent by up to 20 %. Furthermore, they showed that decreasing model resolution from 25 m to 1000 m increased snow water equivalent by up to 10 %. Lafaysse et al. (2017) developed a multi-physical ensemble system to estimate the uncertainty in modeled snow height, density and albedo resulting from different physical parameterizations within a snow-cover model. Raleigh et al. (2015) investigated how different error types, magnitudes and distributions of meteorological input parameters influenced simulated snow water equivalent, ablation rates, snow disappearance and ablation. They employed a global sensitivity analysis based on variance decomposition, which allowed to investigate the fractional contribution of different input parameters on the output of non-linear models. Sauter and Obleitner (2015) performed a similar analysis to explore the influence of input uncertainty on surface-energy balance components of snow cover models. Günther et al. (2019) investigated the sensitivity of snow water equivalent at a field site in Austria to different sources~~ depth or SWE were estimated from meteorological input uncertainty (e.g. Bellaire et al., 2011; Côté et al., 2017; Lapo et al., 2015; Raleigh et al., 2015; Sauter and Obleitner, 2015), different model setups (Günther et al., 2019; Schlögl et al., 2016) or different physical model assumptions (Günther et al., 2019; Lafaysse et al., 2017). Uncertainties from meteorological input had the highest impact on SWE (Günther et al., 2019). For most applications, such as snow hydrology or glacier mass balance, these target variables and time scales are sufficient. However, for snow instability assessment and avalanche formation the relevant time scales are shorter (days to weeks) and snow stratigraphy is a key variable that has to be accounted for (Schweizer et al., 2003a). Indeed, a necessary pre-requisite for dry-snow slab avalanche release is a weak layer within the snow cover below a cohesive slab. Slaughter (2010) therefore estimated the sensitivity of weak layer formation to meteorological input using a snow thermal model. Incoming long-wave radiation was most important, but how input uncertainty impacts the evolution of snow instability

during the entire season was not investigated. Vernay et al. (2015) forced S2M with an ensemble of meteorological input data to estimate the uncertainty in forecasted avalanche hazard from numerical weather prediction models. While meteorological input was assumed to be the main source of uncertainty, ~~i.e. forcing errors, model structure and parameter choice. They showed that forcing errors had the highest impact and parameter choice the lowest. However, no study so far addressed the sensitivity of modeled snow instability estimates~~it was not investigated, how these input uncertainties influenced snow stability in more detail.

We therefore investigated how meteorological input uncertainty influenced modeled snow stability employing a global sensitivity analysis. SNOWPACK was forced with meteorological input of an automatic weather station from a field site above Davos, Switzerland and biases were introduced to the meteorological data. We performed simulations for the winter season 2016-2017, when one weak layer persisted for the entire season and affected snow stability in the region of Davos. We analyzed modeled snow instability metrics related to this weak layer in three steps: we independently investigated the influence of meteorological input uncertainty during three periods of a) weak layer formation, b) slab formation, and c) weak layer and slab formation.

The paper is organized as follows. Section 2 provides an overview of the study site and the simulations with SNOWPACK. This is followed by the description of the uncertainties introduced to the model and the global sensitivity analysis. In Section 3, we first shortly present the winter evolution. Then, the sensitivity of modeled slab and weak layer properties to uncertainties in meteorological input is analysed for two different days: immediately after burial of the weak layer (Section 3.2.1) and for a day with high avalanche activity (Section 3.2.2). Eventually, the evolution of snow stability was analysed with respect to its sensitivity to input uncertainties during the three different periods (Section 3.3). Specific points are finally discussed in Section 4.

2 Methods

2.1 Study site and data

We used data from the field site Weissfluhjoch (WFJ), located in the eastern Swiss Alps above Davos, at an elevation of 2536 m a.s.l. The WFJ site is equipped with an automatic weather station (AWS), which provides the necessary meteorological input to the snow cover model. In addition, traditional snow profiles ~~and stability tests were conducted weekly. Furthermore, we also calculated the Avalanche Activity Index (AAI) based on visual avalanche observation from the region of Davos (about 360 km^2), which were compiled by the avalanche warning service at the SLF. The AAI is the weighted sum of all observed avalanches, where weights are assigned according to avalanche size (Schweizer et al., 2003b)~~were conducted on a weekly basis according to Fierz et al. (2009) (Figure 1a). The winter season 2016-2017 was selected for this study, since the snowpack was marked by a prominent weak layer at about 40 cm from the ground (dark blue colors in Figure 1a) and pronounced avalanche activity on 9 March 2017. The weak layer formed between mid November 2016 and beginning of January 2017 at the surface of the shallow snowpack. For the analysis we will focus on the formation and evolution of this particular layer and its effect on snow stability for the period of high avalanche activity on 9 March 2017. We also calculated the Avalanche Activity

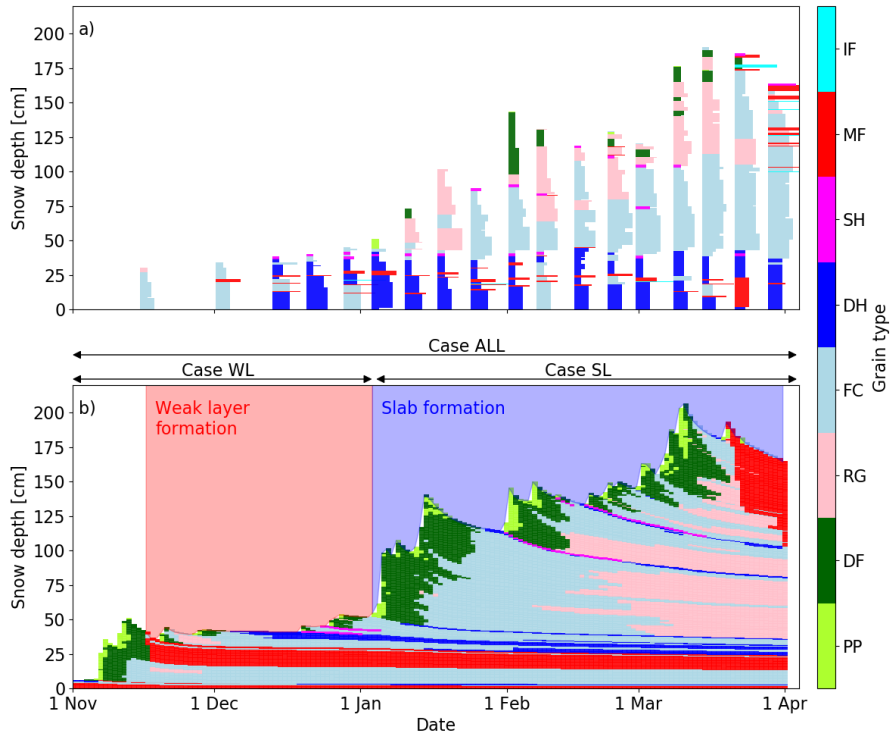

Figure 1. (a) Manually observed snow profiles at the Weissfluhjoch field site for winter season 2016-2017. (b) Reference run simulated with SNOWPACK for winter season 2016-2017 at the WFJ field site above Davos, Switzerland. Shown is the temporal evolution of simulated snow stratigraphy. Colors indicate grain type, i.e. precipitation particles (PP), decomposing and fragmented precipitation particles (DF), rounded grains (RG), faceted crystals (FC), depth hoar (DH), surface hoar (SH), melt forms (MF) and ice formations (IF). Red colored period refers to weak layer formation, blue colored period to slab formation. Arrows indicate different scenarios for which uncertainties were introduced into meteorological model input.

Index (AAI) based on visual avalanche observations from the region of Davos (about 360 km^2), which were compiled by the avalanche warning service at the SLF. The AAI is the weighted sum of all observed avalanches, where weights are assigned according to avalanche size (Schweizer et al., 2003b).

2.2 SNOWPACK

We performed simulations with the snow cover model SNOWPACK version v1473 (e.g. Lehning et al., 2002). SNOWPACK was driven with meteorological data from the AWS at WFJ, including precipitation (P), air temperature (TA), relative humidity (RH), wind velocity (VW), incoming shortwave (ISWR) and longwave (ILWR) radiation. For the reference run we used data from the quality controlled data set at WFJ (WSL Institute for Snow and Avalanche Research SLF, 2015). ~~For the sensitivity analysis, we introduced uncertainties to the meteorological input.~~ SNOWPACK calculated the absorbed shortwave radiation

from modeled surface albedo, not from measured data. Furthermore, data on measured snow ~~height~~ depth and snow surface temperature was explicitly excluded in the configuration. The snow surface temperature was estimated from energy fluxes using Neumann boundary conditions at the snow-atmosphere interface (Bartelt and Lehning, 2002; Lehning et al., 2002). A constant geothermal heat flux of 0.06 W m^{-2} was assumed at the bottom of the snowpack (Davies and Davies, 2010; Pollack et al., 1993). The time step for the simulation was 15 min and output was written every 24 h.

The sensitivity analysis focused on weak and slab properties, as well as modeled snow stability. In particular, the skier stability index ~~SK_{38}~~ SK38 and the critical crack length r_c were analyzed. We focused on the weak layer that formed between 16 November 2016 and 2 January 2017 (see red area in Figure 1b). Since SNOWPACK produces considerably more layers than observed, all simulated snow layers that were deposited between these two dates and consisted of either depth hoar, surface hoar, facets and rounding facets were considered as weak layer, similar to Richter et al. (2019). ~~Then~~ Hence, weak layer thickness D_{wl} was defined as the thickness of all layers consisting of either facets, depth hoar or surface hoar, which were deposited between these two dates. The percentage of facets (% facets), was defined as D_{wl}, divided by the total thickness of all layers which were deposited between these two dates (see Section 3.2.1). Then, weak layer properties were obtained by a thickness-weighted average $\bar{y}$ of the layer properties y_i:

$$\bar{y} = \frac{\sum y_i \, d_i}{\sum d_i}, \tag{1}$$

where d_i is the thickness of the simulated layer i. In analogy, slab properties were calculated from all layers above the weak layer, independent of grain type (see green area in Figure 1~~).~~ b). Slab thickness D_{sl} was defined as the thickness of all slab layers.

The ~~SK_{38} was calculated~~ SK38 was calculated for each simulated snow layer from layer properties of flat field simulations, which were extrapolated to a 38 ° slope according to Jamieson and Johnston (1998)

$$\mathrm{SK38} = \frac{\tau_p}{\tau_s + \Delta\tau}, \tag{2}$$

with the shear strength of the weak layer τ_p, the shear stress due to slab weight $\tau_s = \rho_{sl} g D_{sl} sin(38°) cos(38°)$, the average slab density ρ_{sl}, the slab thickness D_{sl}, the gravitational acceleration g, and the additional shear stress acting on the weak layer due to the weight of a skier $\Delta\tau$. The additional shear stress is modeled as a line load (Föhn, 1987) and for a 38 ° slope, it simplifies to $\Delta\tau = 155/D_{sl}$ m Pa (Monti et al., 2016). Parameterizations for shear strength for different grain types were derived based on shear frame measurements (see Table 8 in Jamieson and Johnston, 2001) and implemented into SNOWPACK. For surface hoar, the shear strength was calculated according to Lehning et al. (2004). Details on shear strength parameterization in SNOWPACK were described by Richter et al. (2019).

The critical crack length was calculated for each simulated snow layer from modeled layer properties using the improved parameterization suggested by Richter et al. (2019):

$$r_c = \sqrt{F_{wl}} \sqrt{E' D_{sl}} \sqrt{\frac{2\tau_p}{\sigma_n}}, \tag{3}$$

with the plane strain elastic modulus of the slab $E' = \frac{E}{(1-\nu^2)}$, the Poisson's ratio of the slab $\nu = 0.2$, and the normal stress $\sigma_n = \rho_{sl} g D_{sl}$ acting on the weak layer due to the overlying slab. The elastic modulus of the slab, E, was related to the slab density by a power law fit to the data collected by Scapozza (2004):

$$E = 5.07 \times 10^9 \left(\frac{\rho_{sl}}{\rho_{ice}} \right)^{5.13} \text{Pa}, \tag{4}$$

The Richter et al. (2019) introduced the correction factor F_{wl} was introduced by Richter et al. (2019): to replace two variables of the original parameterization (Gaume et al., 2017), which were not well defined in SNOWPACK. The factor F_{wl} accounts for weak layer density and grain size and considerably improved the r_c parameterization, and it yields lower values of r_c for layers with larger grains (Richter et al., 2019).

$$F_{wl} = 4.66 \times 10^{-9} \left(\frac{\rho_{wl}\, gs_{wl}}{\rho_{ice}\, gs_0} \right)^{-2.12} \text{m Pa}^{-1}, \tag{5}$$

with the weak layer density ρ_{wl}, the weak layer grain size gs_{wl}, the density of ice $\rho_{ice} = 917\,\text{kg m}^{-3}$ and the reference grain size $gs_0 = 0.00125\,\text{m}$. SK38 an r_c were calculated for each of the weak layers as defined above and thickness-weighted mean instability metrics $\overline{\text{SK38}}$ and $\overline{r_c}$ were determined from all weak layers (Eq. (1)).

2.3 Forcing uncertainties

Uncertainties in the measured meteorological data (Table 1) should reflect uncertainties arising from interpolating meteorological data or weather forecast models. Therefore, uncertainties were introduced based on the values suggested by Raleigh et al. (2015). Uncertainties can be seen as a systematic bias with a given range and distribution. For a given time series, a bias b was randomly chosen for each variable and then that single value applied to the variable for the entire period. The probability distributions of the biases were described by mean (normal: 1, lognormal: 20) and standard deviation (normal: 1, lognormal: 0.5) and then scaled within the given ranges. The bias b was added to the forcing F as $F' = F + b$ for an additive bias and $F' = F(1+b)$ for a multiplicative bias. Raleigh et al. (2015) proposed a multiplicative bias for precipitation (P) and an additive bias for air temperature (TA), relative humidity (RH), wind velocity (VW) and incoming longwave radiation (ILWR). For incoming shortwave radiation (ISWR) we chose a multiplicative bias using a range of 40 % according to the findings of Helbig and Löwe (2012). Biases resulting in non-physical forcing values were filtered to a physical range (e.g. RH was filtered within a range of [0,100] %). With the given ranges and distributions (Table 1), biases can be interpreted as differences typically observed within a distance of about 2 km and an elevation range of about 200 m. For example, around 68 % of the simulations have a bias in air temperature of -1 K to +1 K, which cover temperature differences within an elevation band of around 200 m. Uncertainties in P will yield rather shallow or rather thick snowpacks as typically observed for wind-exposed or wind-sheltered slopes.

In the reference run we used the data from the AWS at WFJ to drive the simulations. Then biases were introduced to the input data using three different scenarios. First, we introduced biases during weak layer formation up to the date when the weak layer was covered with new snow . from 1 October 2016 to 2 January 2017. The subsequent slab formation process from 3

Table 1. Input uncertainties introduced as bias b to meteorological forcing.

Forcing F	Distribution	Range	Unit	Perturbed forcing F'
P	Lognormal	[-75,+300]	%	F' = F(1 + b)
TA	Normal	[-3.0,+3.0]	°C	F' = F + b
RH	Normal	[-25,+25]	%	F' = F + b
VW	Normal	[-3.0,+3.0]	m s^{-1}	F' = F + b
ISWR	Normal	[-40,+40]	%	F' = F(1 + b)
ILWR	Normal	[-25,+25]	W m^{-2}	F' = F + b

January 2017 to 1 April 2017 occurred under the same conditions as in the reference run. We refer to this first scenario as case WL (Figure 1b). Second, meteorological conditions during the period of weak layer formation until 2 January 2017 were identical to those of the reference run, while uncertainties were introduced during the period of slab formation after 3 January 2017 (case SL). Third, we introduced uncertainties to meteorological forcing during the entire simulation period (case ALL). For each scenario, ~~14,000 simulations were performed~~a unique set of quasi-random biases was introduced.

~~Reference run simulated with SNOWPACK for winter season 2016-2017 at the WFJ field site above Davos, Switzerland. Shown is the temporal evolution of simulated snow stratigraphy. Colors indicate grain type, i.e. precipitation particles (PP), decomposing and fragmented precipitation particles (DF), rounded grains (RG), faceted crystals (FC), depth hoar (DH), surface hoar (SH), melt forms (MF) and ice formations (IF). Red colored period refers to weak layer formation, blue colored period to slab formation. Arrows indicate different scenarios for which uncertainties were introduced into meteorological model input.~~

2.4 Global sensitivity analysis

Several studies have shown the advantages of considering co-existing sources of uncertainty by using a global sensitivity analysis rather than varying one input factor at a time while keeping all others fixed (Raleigh et al., 2015; Sauter and Obleitner, 2015). Following their approach, we employed a global sensitivity analysis to analyze the influence of input uncertainty to modeled snow instability. Sobol' (1990) suggested a robust method for nonlinear models based on variance decomposition. The total-order sensitivity index ~~(S_{Ti}) was calculated as:~~

$$S_{Ti} = \frac{E\left[V(\mathbf{Y}|\mathbf{X}_{\sim i})\right]}{V(\mathbf{Y})} = 1 - \frac{V\left[E(\mathbf{Y}|\mathbf{X}_{\sim i})\right]}{V(\mathbf{Y})},$$

~~where E is the expectation operator, V is the variance operator, $\mathbf{Y}$ is the model output and $\mathbf{X}_{\sim i}$ are all input parameters except $\mathbf{X}_i$. In our study,~~ S_{Ti} describes the variance in output variables $\mathbf{Y}$, i.e. snow properties, ~~$\mathbf{Y}$~~ due to uncertainties ~~,~~introduced to a specific meteorological input $\mathbf{X}_i$, while including interactions with other forcing errors:

$$S_{Ti} = \frac{E\left[V(\mathbf{Y}|\mathbf{X}_{\sim i})\right]}{V(\mathbf{Y})} = 1 - \frac{V\left[E(\mathbf{Y}|\mathbf{X}_{\sim i})\right]}{V(\mathbf{Y})}, \quad (6)$$

where E is the expectation operator, V is the variance operator, $\mathbf{Y}$ is the model output and $\mathbf{X}_{\sim i}$ are all input parameters except $\mathbf{X}_i$. Values for S_{Ti} range from 0 ~~to 1. For a perfect additive model, the sum of S_{Ti} is equal~~ (no sensitivity) to 1 ~~, otherwise it is greater than 1.~~ (one-to-one sensitivity).

To efficiently compute S_{Ti}, a quasi-random set of input uncertainties was generated (Saltelli and Annoni, 2010; Saltelli et al., 2010). For this, two independent matrices of input uncertainties $\mathbf{A}$ and $\mathbf{B}$ were defined~~with the~~. The elements a_{ji} and b_{ji} of the two independent matrices $\mathbf{A}$ and $\mathbf{B}$ thus consist of biases for the input variables randomly picked from the ranges and distributions shown in Table 1. The subscript i ranges from one to the number of parameters k, in our case $k = 6$ is the number of forcings F (see Table 1). The subscript j ranges from one to the number of samples N. The calculation of S_{Ti} required the perturbation of parameters, so a third matrix $\mathbf{A}_B^{(i)}$ was introduced, where all columns were taken from $\mathbf{A}$, except for the ith column, which was taken from $\mathbf{B}$, resulting in a $kN \times k$ matrix. From Eq. (6) , S_{Ti} can be computed as:

$$S_{Ti} = \frac{\frac{1}{2N}\sum_{j=1}^{N}\left[f(\mathbf{A})_j - f\left(\mathbf{A}_B^{(i)}\right)_j\right]^2}{V(\mathbf{Y})}, \tag{7}$$

where $f(\mathbf{A})$ is the output variable evaluated on the $\mathbf{A}$ matrix and $f(\mathbf{A}_B^{(i)})$ is the output variable evaluated on the $\mathbf{A}_B^{(i)}$ matrix. For the calculation of S_{Ti}, we generated $N(2k+2)$ samples, with $N = 1000$ base samples, resulting in 14,000 simulations for each of the three applied scenarios.

3 Results

3.1 Winter evolution

The winter started with a snow storm accumulating around 50 cm of snow at the beginning of November 2016 (Figure 1). A melt-freeze crust subsequently formed at the snow surface due to high air temperatures between 16 November 2016 and 19 November 2016 at around 25 cm from the ground (Figure 1b). This crust was also reported in manually observed snow profiles (~~not shown~~Figure 1a). Until 2 January 2017, 20 cm of snow accumulated above the crust (Figure 1). As the weather was mostly clear, the shallow snowpack was subject to strong temperature gradients during that period. The snow above the crust transformed into a weak layer of faceted crystals and depth hoar, which persisted throughout the entire season 2016-2017. This layer was visible in the simulated stratigraphy between 25 cm and 35 cm. After 2 January 2017, another 50 cm of snow accumulated, such that the snow ~~height~~ depth increased from 50 cm to 100 cm within two days. Several small snow storms followed until a maximum snow ~~height~~ depth of about 200 cm was reached on 10 March 2017. Although the snow ~~height~~ depth only increased around 50 cm between 4 March 2017 and 10 March 2017, the peak of avalanche activity was observed by the end of this precipitation period during 9 March (Figure 2a). Many very large avalanches released during this period. Many avalanches in the region of Davos entrained the whole snowpack so that the ground and rocks were visible on the bed surface (Figure 2b). As there were no fracture line profiles recorded, we cannot know in which weak layer the primary failure occurred. Since the weak layer that had formed in December 2016 was the most prominent persistent weak layer within the snowpack

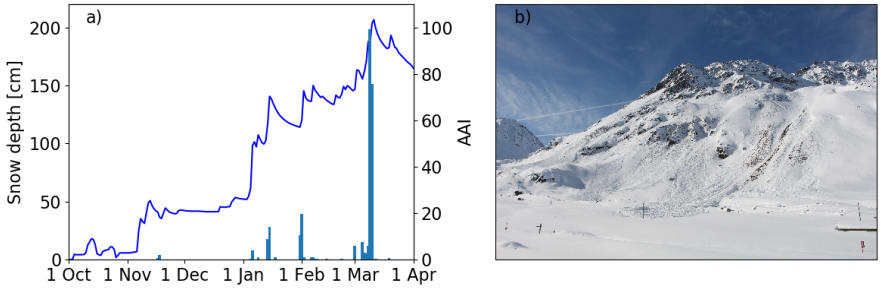

Figure 2. (a) Evolution of modeled snow depth (full line) for winter season 2016-2017 at the WFJ field site above Davos, Switzerland and avalanche activity index (AAI) observed in the region of Davos (blue bars). (b) Avalanches that released during the cycle of 9-10 March 2017, in the valley of Dischma, Davos (picture taken on 15 March 2017). Often the ground or rocks are visible on the bed surface. This was a typical phenomenon for the winter season 2016-2017 due to the old snow problem.

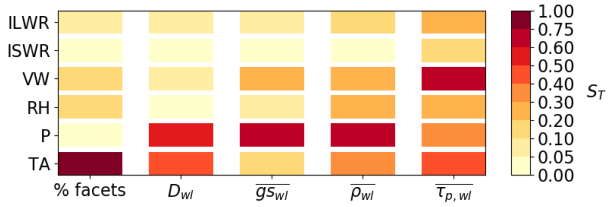

Figure 3. Total sensitivity index of weak layer variables on meteorological input uncertainty on 2 January 2017. Weak layer variables are the proportion of faceted layers (% facets), weak layer thickness (D_{wl}), weak layer grain size ($\overline{gs_{wl}}$), weak layer density ($\overline{\rho_{wl}}$) and weak layer shear strength ($\overline{\tau_{p,wl}}$).

(Figure 1) this weak layer may have been the critical weakness. However, it is also possible that the primary failure occurred between new snow and old snow surface and then stepped down and entrained much of the old snowpack.

3.2 Properties of weak layer and slab

To quantify the influence of input uncertainty on slab and weak layer properties for the three cases, we focused on two specific points in time: 2 January 2017 when we investigated weak layer properties before burial and 9 March 2017 when avalanche activity peaked in the region of Davos (Heck et al., 2019).

3.2.1 2 January 2017

~~Total sensitivity index of weak layer variables on meteorological input uncertainty on 2 January 2017. Weak layer variables are the proportion of faceted layers (% facets), weak layer thickness (D_{wl}), weak layer grain size ($\overline{gs_{wl}}$), weak layer density ($\overline{\rho_{wl}}$) and weak layer shear strength ($\overline{\tau_{p,wl}}$).~~

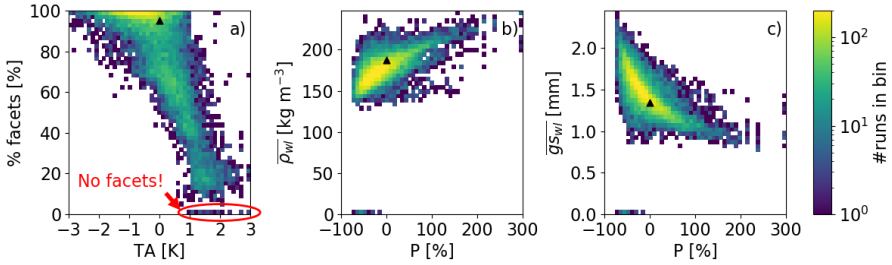

Figure 4. (a) Proportion of faceted layers within the weak layer with uncertainty in air temperature (TA) on 2 January 2017. (b) Density (~~ρ_{wl}~~ $\overline{\rho_{wl}}$) and (c) grain size (~~gs_{wl}~~ $\overline{gs_{wl}}$) of faceted layers with uncertainty in precipitation (P). Colors indicate the binned number of simulations. Triangles indicate the reference run. Red ellipse indicates simulations, in which no weak layer formed.

~~Up to~~ We present weak layer and slab properties on 2 January 2017 ~~the weak layers for case SL were~~ with results from the reference run and case WL because up to 2 January 2017 case SL was identical to the reference run and the distributions of input uncertainties were the same for case WL and case ALL~~we used the same bias distributions. We therefore only present results for case WL and the reference run~~.

On 2 January 2017, the percentage of faceted layers was highly sensitive to air temperature, while the thickness of the weak layer was sensitive to both TA and P (Figure 3). Grain size and density of the weak layer were most sensitive to precipitation. Weak layer shear strength on 2 January 2017 was most sensitive to TA, P and VW ($S_T > 0.3$).

In the reference run, 95 % of the layers that had formed between 16 November and 2 January consisted of faceted grains with a mean grain size of 1.3 mm and a density of 188 kg m^{-3} on 2 January 2017 (Triangles in Figure 4). For case WL, 36 % of the 14,000 simulations also predicted that at least 95 % of the layers that had formed between 16 November and 2 January consisted of faceted grains (Figure 4a). In only 0.3 % of the simulations the weak layer did not form at all, i.e. there were no layers of faceted crystals. These simulations were characterized by a positive air temperature bias (red ellipse in Figure 4a). Warmer air temperature yielded less faceted layers within the weak layer and above a bias of $+1^\circ$ C the percentage of faceted crystals occasionally reached 0 %. ~~Overall, the percentage of faceted layers was highly sensitive to air temperature, while the thickness of the weak layer was sensitive to both TA and P (Figure 3). Grain size and density of the weak layer were most sensitive to precipitation.~~ Increasing P led to denser weak layers and smaller grains (Figure 4b,c). Positive biases in P result in thicker snowpacks, as would typically be observed in wind-sheltered locations. In fact, in 76 % of the simulations, the density of the weak layer was lower and in 67 % of the simulations the grain size was larger than in the reference run. Both properties, soft snow (low density) and larger grains are often associated with unstable weak layers (van Herwijnen and Jamieson, 2007). ~~Finally, weak layer shear strength on 2 January 2017 was most sensitive to TA, P and VW ($S_T > 0.3$).~~

3.2.2 9 March 2017

We present weak layer and slab properties on 9 March 2017 by comparing all three cases with results from the reference run.

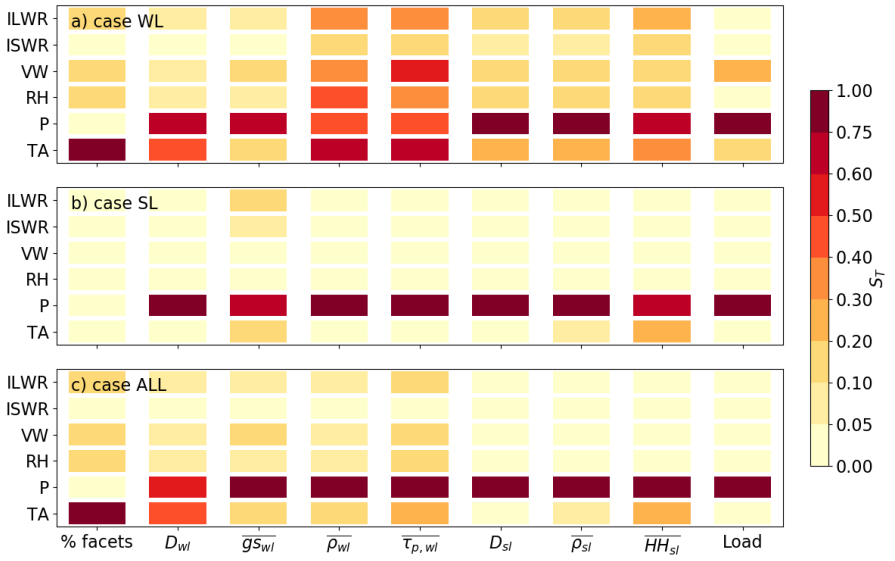

Figure 5. Total sensitivity index of different weak layer and slab variables on meteorological input uncertainty on 9 March 2017 for (a) case WL, (b) case SL and (c) case ALL. Variables are the proportion of facets (% facets), weak layer thickness (D_{wl}), weak layer grain size ($\overline{gs_{wl}}$), weak layer density ($\overline{\rho_{wl}}$), weak layer shear strength ($\overline{\tau_{p,wl}}$), slab thickness (D_{sl}), slab density ($\overline{\rho_{sl}}$), hand hardness index of the slab ($\overline{HH_{sl}}$) and load due to the slab weight (Load).

The total sensitivity indices for case WL on 9 March 2017 were similar to those on 2 January 2017 for D_{wl} and $\overline{gs_{wl}}$. For density and shear strength, all input parameters except ISWR increased to $S_T > 0.3$ (Figure 5a). In contrast, for case SL, weak layer and slab properties were primarily sensitive to P (Figure 5b). Increasing P increased the load on the weak layer and yielded smaller grains and higher weak layer density (Figure 6d,e). For case ALL, uncertainties in P dominated weak and slab properties. Similarly, density and shear strength of the weak layer on 9 March 2017 were mostly sensitive to P, suggesting that the density evolution of the weak layer was determined by the load rather than the original density after burial.

On 9 March 2017, mean weak layer density (325 kg m^{-3}) and mean grain size (1.6 mm) in the reference run had clearly increased compared to 2 January 2017. On top of the weak layer, the reference run simulated a 165 cm thick slab with a mean density of 256 kg m^{-3} corresponding to a load of 4.15 kPa (triangles in Figure 6).

In all three cases, around 66 % of the simulations predicted a weak layer with a lower mean density than in the reference run. The range was smallest for case WL, with ~~ρ_{wl}~~ $\overline{\rho_{wl}}$ ranging from 295 kg m^{-3} to 370 kg m^{-3} and highest for case ALL, with ~~ρ_{wl}~~ $\overline{\rho_{wl}}$ ranging from 240 kg m^{-3} to 401 kg m^{-3} (Figure 6a,d,g). This means that the weak layer density on 9 March 2017 was more influenced by the slab than the original density prior to burial. In contrast, the grain size of the weak layer rather depended on the original grain size. Hence, the dispersion for case ALL was similar to case WL, with ~~gs_{wl}~~ $\overline{gs_{wl}}$ ranging from 1.0 mm to 3.0 mm, whereas ~~gs_{wl}~~ $\overline{gs_{wl}}$ predicted by case SL was similar to the reference run, ranging from 1.6 mm to 2.0 mm (Figure

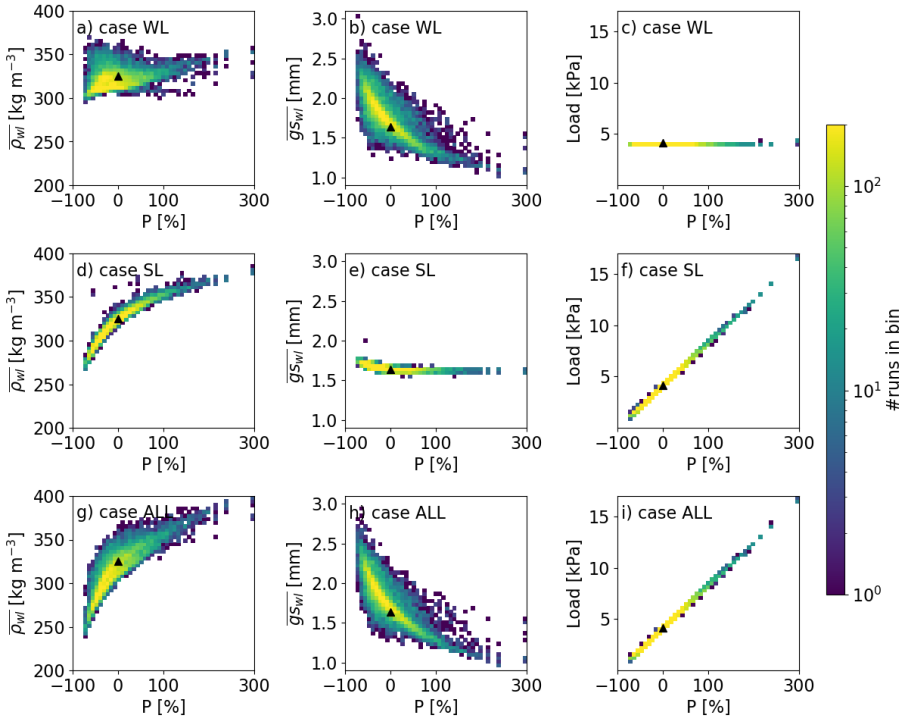

Figure 6. Modeled (a,d,g) weak layer density, (b,e,h) weak layer grain size and (c,f,i) load of the slab with uncertainty in precipitation (P) on 9 March 2017 for (a,b,c) case WL, (d,e,f) case SL and (g,h,i) case ALL. Colors indicate the binned number of simulations. Triangles indicate the reference run.

6b,e,h). In all three cases, around 70 % of the simulations predicted grain sizes larger than the reference run. As expected, the range in slab properties for case WL was minimal on 9 March 2017, e.g. the load of the slab ranged from 4.13 kPa to 4.18 kPa. In contrast, the load for case SL and case ALL varied by a factor of 16, ranging from 1.03 kPa to 16.7 kPa (Figure 6c,f,i). In all three cases, around one third of the simulations predicted a higher slab load than the reference run. Other slab properties, e.g. slab density, did not vary much for case WL, whereas they greatly varied for case SL and case ALL. To sum up, different slab properties strongly influenced the evolution of the weak layers, whereas different weak layers, as expected, did not influence the evolution of the slab.

~~The total sensitivity indices for case WL on 9 March 2017 were similar to those on 2 January 2017 for D_{wl} and gs_{wl}. For density and shear strength, all input parameters except ISWR increased to $S_T > 0.3$ (Figure 5a). In contrast, for case SL, weak layer and slab properties were dominantly sensitive to P (Figure 5b). Increasing P increased the load on the weak layer and yielded smaller grains and higher weak layer density (Figure 6d,e). For case ALL, uncertainties in P dominated weak and slab properties. Similarly, density and shear strength of the weak layer on 9 March 2017 were mostly sensitive to P, suggesting that the density evolution of the weak layer was determined by the load rather than the original density after burial.~~

3.3 Evolution of snow stability

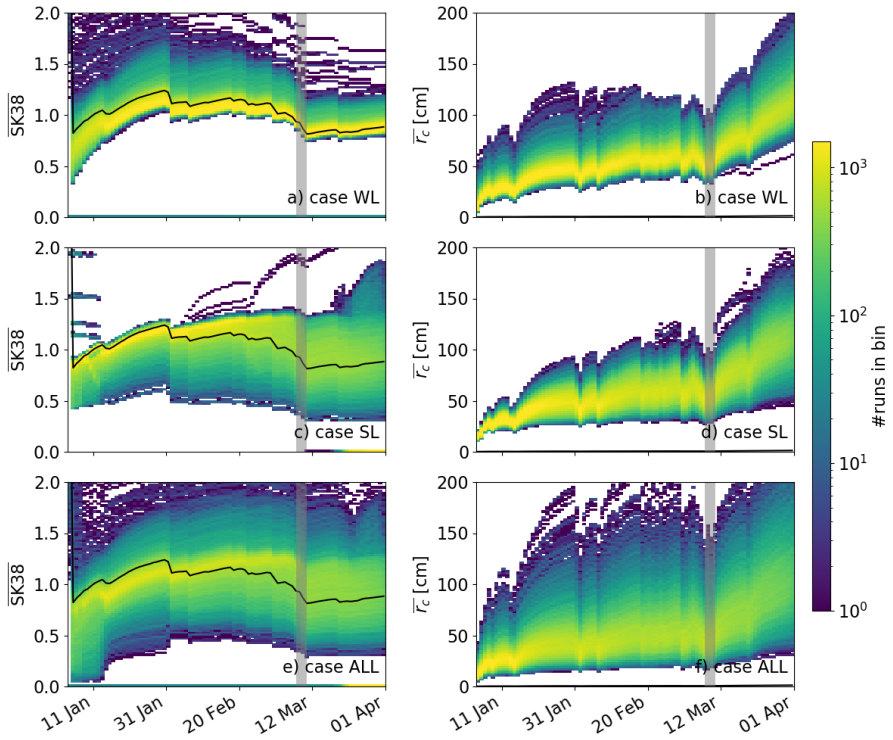

Figure 7. Temporal evolution (January to March 2017) of input uncertainties to modeled skier stability index ~~SK_{38}~~ $\overline{\text{SK38}}$ for (a) case WL, (c) case SL, (e) case ALL and critical crack length ~~r_c~~ $\overline{r_c}$ for (b) case WL, (d) case SL, (f) case ALL. Colors indicate the binned number of simulations. Black lines show the reference run and grey vertical bars highlight the period of high avalanche activity.

~~Evolution of the total sensitivity index S_T for the model output SK_{38} and r_c for case WL, case SL and case ALL (from top to bottom). Grey vertical bars highlight period of high avalanche activity.~~

After burial of the weak layer, snow stability of the reference run, i.e. ~~SK_{38} and r_c~~ $\overline{\text{SK38}}$ and $\overline{r_c}$, initially increased with time (black lines in Figure 7). During periods with precipitation (increases in snow ~~height~~ depth in Figure 1), both indices decreased, whereas during periods without precipitation, both indices increased. However, this increase was very weak for ~~SK_{38}~~ $\overline{\text{SK38}}$. On 30 January 2017, ~~SK_{38}~~ $\overline{\text{SK38}}$ reached a maximum value of 1.24. After that, decreases in ~~SK_{38}~~ $\overline{\text{SK38}}$ during periods with precipitation events were stronger than increases ~~SK_{38}~~ $\overline{\text{SK38}}$ during periods without precipitation. Therefore, an overall decrease was observed for ~~SK_{38}~~ $\overline{\text{SK38}}$ after 30 January 2017, such that ~~SK_{38}~~ $\overline{\text{SK38}}$ reached a minimum value of 0.81 during the period of high avalanche activity (10 March 2017). In contrast, ~~r_c~~ $\overline{r_c}$ increased more prominently during periods without precipitation, such that ~~r_c~~ $\overline{r_c}$ reached a minimum value of 15 cm right after burial and a maximum value of 124 cm by the end of March. During periods with precipitation, ~~r_c~~ $\overline{r_c}$ decreased, e.g. ~~r_c~~ $\overline{r_c}$ decreased just before the period 9 March 2017, such that lower values for ~~r_c~~ $\overline{r_c}$ during the peak of avalanche activity were modeled (indicated by grey vertical bars in Figure

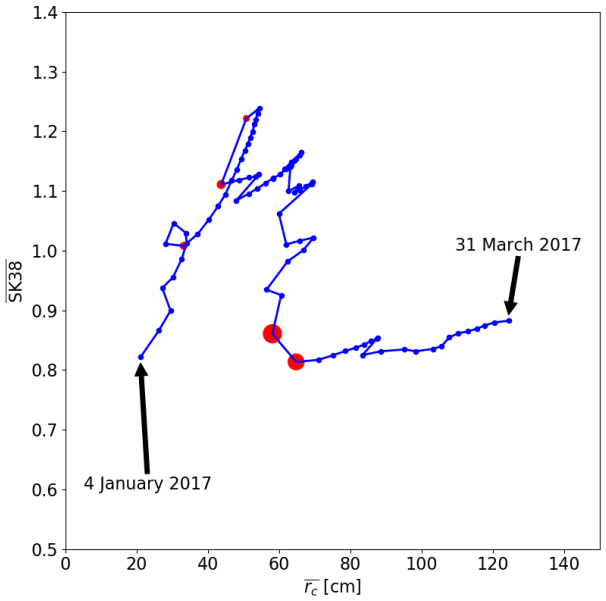

Figure 8. ~~SK_{38}~~ SK38 with ~~r_c~~ $\overline{r_c}$ of the reference run for all days from 4 January 2017 to 31 March 2017. Red circles are days with AAI > 10 and the size of the circles ~~correspond~~ corresponds to the value of AAI.

7). Therefore, days with high avalanche activity coincided with days with small values for ~~r_c~~ $\overline{r_c}$ and small values for ~~SK_{38}~~ SK38 (Figure 8).

Similar to the reference run, ~~SK_{38} and r_c~~ SK38 and $\overline{r_c}$ initially increased for all three cases. After 30 January, an overall decrease in ~~SK_{38}~~ SK38 was observed, while the increase in ~~r_c~~ $\overline{r_c}$ was more pronounced towards the end of the simulation period. During periods with precipitation, decreases in snow stability were observed (Figure 7).

While $\overline{r_c}$ was mostly sensitive to precipitation for case WL, SK38 was highly sensitive to TA (Fig. 9a,b). In contrast, for case SL and case ALL, the total-order sensitivity index clearly highlighted precipitation as the most dominant input parameter for stability indices (Figure 9c-f). Interestingly, the instability metrics were affected in different ways by uncertainties in precipitation. On 9 March 2017, for all cases, increasing precipitation yielded larger critical crack lengths (Figure 10). The strongest increase for $\overline{r_c}$ with P was observed for case ALL (Figure 10d). Whereas SK38 increased with increasing TA for case WL (Figure 10a), it clearly decreased with increasing P for case SL and case ALL (Figure 10c,e). The decrease is a consequence of the more prominent increase in slab load than in shear strength. In fact, the shear strength increased with increasing precipitation by a factor of two while slab load increased with increasing precipitation by a factor of six (not shown).

The range of ~~SK_{38}~~ SK38 was larger in case SL compared to case WL, suggesting that the load due to slab weight had a stronger influence on ~~SK_{38}~~ SK38 than the shear strength of the weak layer. On 9 March 2017 for instance, ~~SK_{38}~~ SK38 ranged from 0.79 to 1.87 for case WL and 0.33 to 1.90 for case SL (Figure 10a,c). This suggests, that different slabs influenced ~~SK_{38}~~

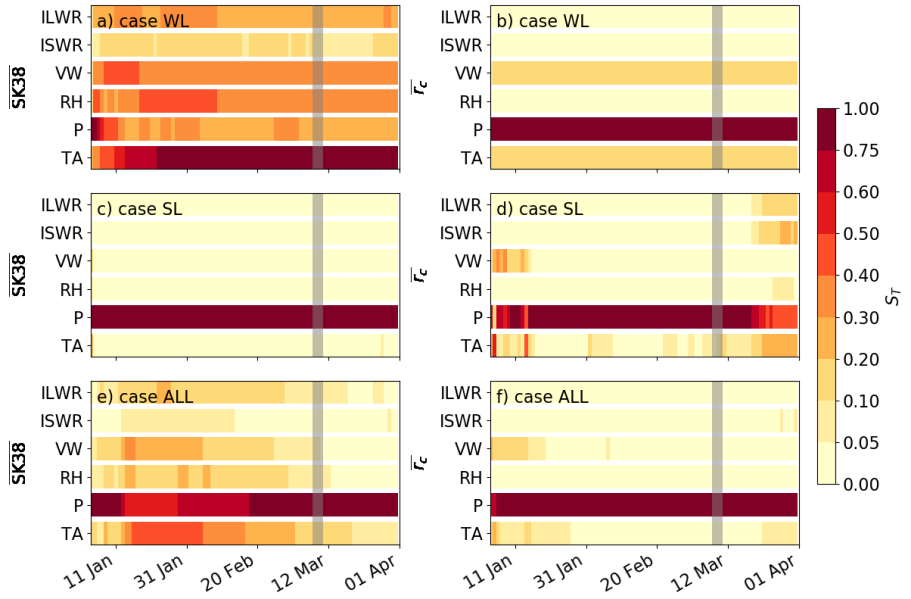

Figure 9. Evolution of the total sensitivity index S_T for the model output $\overline{SK38}$ and $\overline{r_c}$ for case WL, case SL and case ALL (from top to bottom). Grey vertical bars highlight period of high avalanche activity.

$\overline{SK38}$ more than different weak layers, i.e. the slab was more important. Case ALL showed the largest range from 0.32 to 3.05 (Figure 10e). Around one third of the simulations for all cases predicted a ~~SK_{38}~~ $\overline{SK38}$ smaller than that for the reference run with a value of 0.86 (case WL: 44 %, case SL: 36 % and case ALL: 33 %). The spread of ~~r_c~~ $\overline{r_c}$ was similar in case WL and case SL, ranging from around 30 cm to 100 cm on 9 March 2017 (Figure 10b,d). For case ALL, the spread of r_c was larger, ranging from 18 cm to 146 cm on 9 March 2017 (Figure 10f). This suggests that $\overline{r_c}$ was equally impacted by weak layer and slab properties. Around two thirds of the simulations in all three cases predicted a value of ~~r_c~~ $\overline{r_c}$ smaller than in the reference run with a value of 58 cm (case WL: 71 %, case SL: 65 % and case ALL: 69 %). However, only 30 % of the simulations of case WL predicted both, a smaller ~~SK_{38}~~ $\overline{SK38}$ and a smaller ~~r_c~~ $\overline{r_c}$ value on 9 March 2017. For case SL and case ALL, only 6 % and 7 % of the simulations, respectively, predicted lower values for both stability indices. This means that if a simulation yields a smaller ~~SK_{38}~~, ~~r_c~~ $\overline{SK38}$, $\overline{r_c}$ was mostly larger. Stability indices therefore did not respond to the biases in a similar manner.

~~While r_c was mostly sensitive to precipitation, for case WL, SK_{38} was highly sensitive to TA (Fig. 9a,b). In contrast, for case SL and case ALL, the total-order sensitivity clearly highlighted precipitation as the most dominant input parameter for stability indices (Figure 9c-f). Although during precipitation events, r_c temporarily decreased (Figure 7) the load by the slab affected the consolidation of the weak layer as well as the slab layers. A higher load induced higher weak layer strength and a stiffer slab so that r_c increased. On 9 March 2017, for all cases, increasing precipitation yielded larger critical crack lengths (Figure 10). This strongest increase for r_c with P was observed for case ALL (Figure 10d). Whereas SK_{38} increased with increasing TA for case WL (Figure 10a), it clearly decreased with increasing P for case SL and case ALL (Figure 10c,e).~~

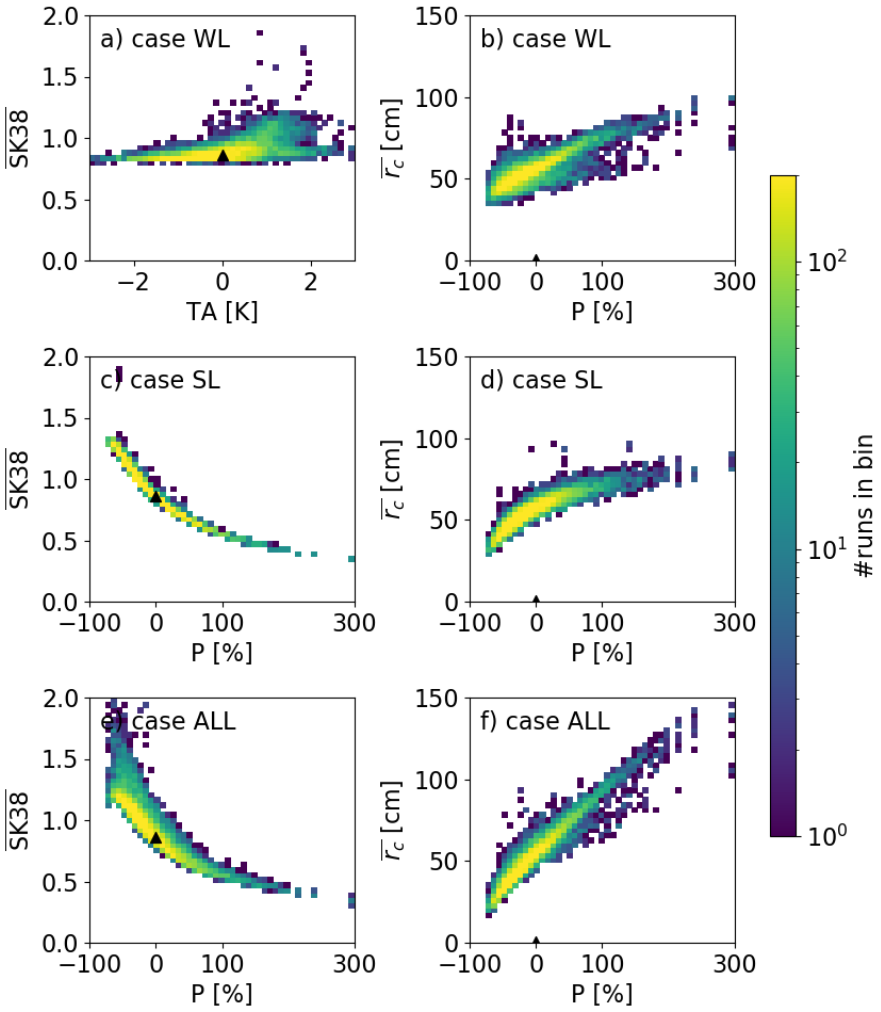

Figure 10. Modeled (a,c,e) ~~skier stability index (SK_{38})~~ $\overline{SK38}$ and (b,d,f) ~~critical crack length~~ $\overline{r_c}$ with uncertainty in most sensitive input parameter, i.e. air temperature (TA) and precipitation (P) on 9 March 2017 for (a,b) case WL, (c,d) case SL and (e,f) case ALL. Colors indicate the number of simulations in each of the 50×50 bins. Triangles indicate the reference run.

~~The decrease is a consequence of the more prominent increase in slab load than in shear strength. In fact, the shear strength increased with increasing precipitation by a factor of two while slab load increased with increasing precipitation by a factor of six (not shown).~~

4 Discussion

We examined the sensitivity of modeled snow stability to meteorological input uncertainty using a global sensitivity analysis approach suggested by Sobol' (1990). To do so, we introduced biases to six meteorological inputs: air temperature, relative humidity, precipitation, wind velocity, incoming short- and long wave radiation, which are all required as input variables by the snow cover model SNOWPACK (Lehning et al., 2002). Among these input parameters, precipitation had the most prominent influence on modeled snow stability. Precipitation influences weak layer and slab properties. Although a positive bias in air temperature reduced the percentage of faceted crystals within the weak layer, in most simulations a weak layer had formed, which may indicate a widespread avalanche problem in the region.

We used biases instead of random uncertainties, as Raleigh et al. (2015) investigated different sources of errors and showed that biases had more influence on model output. For the parameter biases, we used the ranges suggested by Raleigh et al. (2015), who provided a comprehensive overview of typical variations in these parameters in complex topography. The only exception was for ISWR, for which we chose a multiplicative bias rather than a cumulative bias, since we expected bias in ISWR to depend on solar angle. ~~As the radiation balance in snow covered complex topography can lead to large variations in incoming shortwave radiation (Helbig and Löwe, 2012), we used a range of $\pm 40\,\%$~~Introducing a lognormal distribution for the bias in precipitation resulted in unequal proportions relative to the reference run (e.g. Figures 4 and 6). A coefficient of variation for the lognormal distribution was chosen as this reflects typical snow depth patterns observed in mountainous terrain (e.g. Liston, 2004). Hence, relatively more simulations had smaller P values than the reference run. While the snow cover model SNOWPACK has traditionally been forced with measured data from automatic weather stations (Lehning et al., 1999; Monti et al., 2015; Wever et al., 2015), it is increasingly used for spatially distributed model applications either by interpolating measured meteorological data or using output from numerical weather prediction models (Bellaire et al., 2011; Bellaire and Jamieson, 2012; Schlögl et al., 2016). As such, the introduced biases can be seen as potential errors due to the interpolation schemes, or biases in the NWP output. For instance, for air temperature, the variation of $\pm 3\,^{\circ}$ C (Table 1) corresponds roughly to typical errors between NWP output and TA measurements (Bellaire et al., 2017).

In complex terrain, wind induced processes strongly influence snow distribution (Mott and Lehning, 2010). The bias introduced for P agree with the high variations in snow depths, measured at very small scale (Bühler et al., 2015). P had the most significant impact on modeled sensitivity, which may partly be due to the high magnitude of bias (Raleigh et al., 2015). These results have implications for spatial snow cover modeling, which is increasingly applied in avalanche forecasting (Bellaire et al., 2017, 2011; Morin et al., 2020; Lafaysse et al., 2017; Vernay et al., 2015). Indeed, our results suggest that if we want to obtain realistic spatial patterns, we need to adequately model snow distribution in mountainous regions. This is not an easy task, as snow distribution is very complex (Grünewald et al., 2010; Helbig and van Herwijnen, 2017; Kirchner et al., 2014; Reuter et al., 2016). Since the mountain snow cover is largely shaped by snow transport by wind, adequate modeling can only be achieved through computationally expensive snow drift modeling (Gerber et al., 2018; Mott and Lehning, 2010; Vionnet et al., 2014). While from an operational point of view, high resolution modeling (resolution of several meters) on large domains

is presently out of reach, alternative approaches were suggested (e.g. Helbig et al., 2017; Vögeli et al., 2016; Winstral et al., 2002).

~~Previous snow sensitivity studies typically focused on snow depth or snow water equivalent by introducing model uncertainties during the entire season (Lapo et al., 2015; Raleigh et al., 2015; Sauter and Obleitner, 2015). For most applications, such as snow hydrology or glacier mass balance, these target variables and time scales are sufficient. However, for snow instability assessment and avalanche formation the relevant time scales are shorter (weeks) and snow stratigraphy is a key variable that has to be accounted for (Schweizer et al., 2003a). Indeed, a necessary pre-requisite for dry-snow slab avalanche release is a weak layer within the snow cover below a cohesive slab.~~

~~Simulations were performed for the field site Weissfluhjoch above Davos, Switzerland, for the winter season 2016-2017. This winter was characterized by a thick persistent weak layer that developed early in the season (December) and likely contributed to a widespread avalanche cycle in the area in March (Figure 2). We thus~~ We investigated the formation and subsequent burial of ~~this~~ a weak layer consisting of faceted ~~grains~~ and depth hoar crystals near the base of the snow cover, often called persistent weak layer (Jamieson and Johnston, 1992; Schweizer et al., 2003a). Such early season weak layers are often widespread and associated with poor stability for most of the season. ~~Grain size and hardness are important parameters to identify persistent weak layers and evaluate snow stability (e.g. Schweizer and Jamieson, 2007; van Herwijnen and Jamieson, 2007).~~ Results from our sensitivity analysis thus showed that the formation of the weak layer was mostly influenced by precipitation and air temperature early in the season (Figure 3). This comes as no surprise since both the parameters directly affect the temperature gradient across the snowpack, which is the most important driver for the formation of facets and depth hoar (Birkeland, 1998; Miller and Adams, 2009; Staron et al., 2012). Our results also show that the formation of persistent weak layers is rather robust. Indeed, in only 0.3 % of the simulations no weak layer developed, suggesting that even within the range of meteorological input we used, if a prolonged dry weather period occurs after the first snowfall, such weak layers will generally form. Only warm weather can prevent the formation of a weak layer during a prolonged dry weather period, which is generally found at lower elevations. Our results suggest that spatial snow cover modeling can be used to predict the elevation range for weak layers. This result agrees with Horton et al. (2015) who examined how variability in meteorological fields from numerical weather prediction models across elevations resulted in reasonable predictions of surface hoar formation. However, we only looked at one type of weak layer. The formation and subsequent burial of surface hoar might be more sensitive to other meteorological parameters, such as wind speed (Stössel et al., 2010). In fact, Slaughter (2010) investigated the sensitivity of near-surface faceting and surface hoar formation at mid-day and mid-night to input parameters using a snow thermal model. He found incoming long-wave radiation to be the most dominant input parameter, although they did not investigate the sensitivity to precipitation.

Grain size and hardness are important parameters to identify persistent weak layers and evaluate snow stability (e.g. Schweizer and Jamieson, 2007; van Herwijnen and Jamieson, 2007). The low sensitivity of weak layer grain size to air temperature and radiation (Figure 4) during the weak layer formation period was somewhat surprising, since both these parameters are highly relevant for the energy input at the snow surface and thus snow surface temperature and temperature gradients across the snowpack. However, the weak layer formed in December, when the energy balance at the snow surface is generally negative (i.e. surface cooling), as days are very short and incoming short-wave radiation is very low. Even with

positive air temperature, the snow surface often stays well below zero, except on very steep south-facing slopes (higher incoming short-wave radiation), or when there is a thick cloud cover (higher incoming long-wave radiation). Since there was generally only limited cloud cover in December 2016 (low incoming long-wave radiation), and the simulations were performed for a flat field site (low incoming short-wave radiation), we believe our results are plausible. Hence, weak layer grain size was mostly sensitive to uncertainties in precipitation, as thinner snow covers generally have a lower density (less settlement) and experience larger temperature gradients. Weak layer shear strength was sensitive to uncertainties in wind velocity and air temperature (Figure 4). Shear strength in SNOWPACK is a function of grain type and density. As new snow density in SNOWPACK depends on VW and TA, we believe that weak layer shear strength depended on these variables for case WL on 2 January 2017. In fact, weak layer shear strength increased with increasing VW and increasing TA (not shown). As different weak layers on 2 January do not necessarily react exactly the same to the same slab, there were some changes in S_T between 2 January and 9 March. Indeed, harder and denser weak layers will settle less than soft low density weak layers.

We focused on two metrics of snow instability, namely ~~SK_{38}~~ SK38 (Eq. (2)) and r_c (Eq. (3)). These metrics relate to both failure initiation (~~SK_{38}~~SK38) and crack propagation (r_c), two fundamental processes required for avalanche release (Reuter and Schweizer, 2018; van Herwijnen and Jamieson, 2007). Given our current understanding of snow stability, critical weak layers require both a low failure initiation propensity and a low crack propagation propensity (Reuter and Schweizer, 2018). While both these indices have been validated (Schweizer et al., 2006; Richter et al., 2019), thus far no threshold values exist that separate stable from unstable snow conditions adapted for use in SNOWPACK. As such, we compared these stability indices to the reference run to determine if the introduced biases resulted in a more stable or a less stable snowpack, with a particular focus on 9 March 2017 when avalanche activity in the regions of Davos peaked (Fig 2).

To better assess the role of slab and weak layer properties with respect to snow instability, we used three scenarios where we varied meteorological input only during the weak layer formation period, only during the slab formation period and during the entire period. These three scenarios clearly highlighted that weak layer and slab formation are sensitive to different meteorological parameters and can influence snow instability in very different ways (Figures 5 and 9). With higher precipitation during the slab formation period r_c generally increased, whereas ~~SK_{38} decreased~~ SK38 decreased (Figure 10c,d). Precipitation determined slab load and the consolidation of slab and weak layers. More precipitation resulted in thicker slabs which typically have a higher density, hardness and stiffness (van Herwijnen and Jamieson, 2007; van Herwijnen et al., 2016). Furthermore, due to higher slab load, the weak layer shear strength increased~~, resulting~~ . Both, stiffer slab and higher weak layer shear strength resulted in higher values for r_c. This is in line with other parametric studies on snow instability showing that slab properties substantially affect snow instability (Gaume et al., 2017; Reuter and Schweizer, 2018; Schweizer and Reuter, 2015). ~~Furthermore, our results suggest that even if a persistent weak layer forms at the start of the season, the remainder of the winter season can still have a profound effect on the overall evolution of snow instability.~~

In contrast, ~~the decrease in SK_{38} is aconsequence of the more prominent~~ SK38 decreased during precipitation due to the increase in slab load and slightly increased during periods without precipitation (Figure 7a,c,e) due to the lagged increase in weak layer shear strength (Jamieson et al., 2007). However, the increase in slab load ~~than in shear strength.~~ was more prominent than the increase in weak layer shear strength, resulting in an overall decrease in SK38 and values for SK38 remained low

towards end-March 2017 (Figure 7 and 8). For the same reason, SK38 was affected differently than r_c with uncertainties in precipitation. Hence, SK38 decreased with increasing P (Figure 10c) during the slab formation period. In fact, ~~the shear strength increased with increasing precipitation by a factor of two, while slab load increased with increasing precipitation by a factor of six~~ with increasing P, the slab load by 9 March had increased three times as much as weak layer shear strength (not shown). With increasing slab thickness the skier stress on the weak layer decreases and skier triggering becomes unlikely. ~~SK_{38}~~ SK38 can no longer be used to assess skier triggering (Schweizer et al., 2016). Instead, other stability indices should be considered, e.g. the natural stability index. However, the denominator in Eq. (2) is dominated by the shear stress due to the load of the slab for thicker slabs. Hence ~~SK_{38}~~ SK38 approaches the natural stability index for slab thicknesses above approximately one meter. During the precipitation event of 9 March 2017, these strength-over-stress approaches reach a small value, meaning that a failure is easy to initiate. Even towards the end of March 2017, ~~SK_{38}~~ SK38 and the natural stability index (not shown) remain very low, which is rather counter-intuitive regarding failure initiation.

In the context of climate change, Castebrunet et al. (2014) suggested a decrease in avalanche activity for the Alps and an increase in wet-snow avalanche activity during winter at high elevations. Martin et al. (2001) assumed that avalanche hazard (number of days with moderate or high avalanche hazard) decreased with increasing TA. Our study also allows assessing the effect of increasing temperature on snow instability. With increasing TA during the formation of the weak layer, the weak layer will get stronger, meaning higher density and smaller grain size. This results in an overall more stable snowpack. However, in our case study only 0.3 % of the simulations, no weak layer formed at all. We therefore expect, that instabilities due to persistent weak layers will continue to challenge avalanche forecasting. This is in particular of interest, since about 70 % of 186 skier-triggered avalanches were released in weak layers of persistent grain types, i.e. surface hoar, faceted crystals, and depth hoar (Schweizer and Jamieson, 2001). ~~The primary driver~~ Furthermore, the primary driver of snow instability after weak layer formation was precipitation~~,~~. With climate change, extreme events may become more frequent, e.g. prolonged dry periods - favoring the formation of weak layers - may alternate with more extreme precipitation events (CH2018, 2018) - with partly opposing effects on our snow instability metrics.

5 Conclusions

We investigated the sensitivity of two modeled snow instability metrics for a weak layer consisting of faceted and depth hoar crystals on meteorological input uncertainty by employing a global sensitivity analysis. We evaluated three scenarios, in which uncertainties were introduced during the weak layer formation period, the slab formation period and the whole winter season. This approach allowed to independently investigate the effects on weak layer and slab properties, which both contribute to snow stability.

The process of weak layer formation was very robust as in most simulations persistent grain types formed. However, weak layer properties strongly depended on meteorological conditions during the formation period. While ~~weak layer grain size was sensitive to precipitation, weak layer density and shear strength were also sensitive to other input parameters during the period of weak layer formation, such as air temperature , relative humidity and wind velocity. The smaller the strength of the weak~~

layer initially was, the weaker the snowpack stayed later on. we only investigated one winter with a rather thin snow cover, we expect this to hold also for a thicker snow cover, as the upper layers will experience strong temperature gradients. Hence, accurate meteorological input is important for forecasting the spatial distribution of weak layers and how weak they really are, since this helps assessing snow instability later in the season.

Once a weak layer had formed, its propertiesboth, slab and weak layer properties, were strongly sensitive to uncertainties in precipitation during the slab formation period. While the grain size of the weak layer was more determined by the initial grain size before burial, the weak layer density and accordingly, weak layer shear strength were mostly determined by the load of the slab. Moreover, slab properties were largely sensitive to precipitation during slab formation. Therefore, precipitation was found to be the strongest driver of snow propertiesPrecipitation determined the load and hence, the settling of slab and weak layers. These snow properties, however, influenced modeled snow stability in different ways. For example, While a positive bias in precipitation, which can be found in wind-shaded areas with above-average accumulation, resulted in an overall lower skier stability index and higher critical crack length. Vice versa for areas with below-average snow depth, a higher skier stability index and a lower critical crack length was simulated. Our results suggest that even if a persistent weak layer forms at the start of the season, the remainder of the winter season can still have a profound effect on the overall evolution of snow instability.

As snow deposition in complex terrain substantially varies during storms and given the high sensitivity of stability to precipitation, numerical forecasting of snow stability in 3D terrain will require spatially highly resolved precipitation patterns.

Data availability. Upon acceptance all relevant data will be made available on www.envidat.ch.

Author contributions. BR processed and analyzed the simulations. AH and JS initiated this study. BR prepared the paper with contributions from all co-authors.

Competing interests. The authors declare that they have no conflict of interests.

Acknowledgements. Thanks to Mathias Bavay for helping with SNOWPACK issues, Thomas Kramer for IT support and Henning Löwe for discussions on programming style. Furthermore, we thank Simon Horton, one anonymous referee and the editor Margreth Keiler, who helped us to improve this paper. Bettina Richter has been supported by a grant of the Swiss National Science Foundation (200021_169641).

References

Bartelt, P. and Lehning, M.: A physical SNOWPACK model for the Swiss avalanche warning Part I: Numerical model, Cold Reg. Sci. Technol., 35, 123–145, 2002.

Bellaire, S. and Jamieson, B.: Nowcast with a forecast–snow cover simulations on slopes, Proceedings of International Snow Science Workshop, Anchorage, USA, pp. 172–178, 2012.

Bellaire, S., Jamieson, B., and Fierz, C.: Forcing the snow-cover model SNOWPACK with forecasted weather data, The Cryosphere, 5, 1115–1125, https://doi.org/10.5194/tc-5-1115-2011, 2011.

Bellaire, S., van Herwijnen, A., Mitterer, C., and Schweizer, J.: On forecasting wet-snow avalanche activity using simulated snow cover data, Cold Regions Science and Technology, 144, 28 – 38, https://doi.org/10.1016/j.coldregions.2017.09.013, http://www.sciencedirect.com/science/article/pii/S0165232X17301891, international Snow Science Workshop 2016 Breckenridge, 2017.

Birkeland, K. W.: Terminology and Predominant Processes Associated with the Formation of Weak Layers of Near-Surface Faceted Crystals in the Mountain Snowpack, Arctic and Alpine Research, 30, 193–199, https://doi.org/10.1080/00040851.1998.12002891, 1998.

Brun, E., David, P., and Sudul, M.: A numerical-model to simulate snow-cover stratigraphy for operational avalanche forecasting, J. Glaciol., 38, 13–22, 1992.

Bühler, Y., Marty, M., Egli, L., Veitinger, J., Jonas, T., Thee, P., and Ginzler, C.: Snow depth mapping in high-alpine catchments using digital photogrammetry, The Cryosphere, 9, 229–243, https://doi.org/10.5194/tc-9-229-2015, 2015.

Castebrunet, H., Eckert, N., Giraud, G., Durand, Y., and Morin, S.: Projected changes of snow conditions and avalanche activity in a warming climate: the French Alps over the 2020-2050 and 2070-2100 periods, The Cryosphere, 8, 1673–1697, https://doi.org/10.5194/tc-8-1673-2014, 2014.

CH2018: CH2018 - Climate Scenarios for Switzerland, Technical Report, National Centre for Climate Services, Zurich, ISBN: 978-3-9525031-4-0, 2018.

Côté, K., Madore, J.-B., and Langlois, A.: Uncertainties in the SNOWPACK multilayer snow model for a Canadian avalanche context: sensitivity to climatic forcing data, Physical Geography, 38, 124–142, https://doi.org/10.1080/02723646.2016.1277935, 2017.

Davies, J. H. and Davies, D. R.: Earth's surface heat flux, Solid Earth, 1, 5–24, https://doi.org/10.5194/se-1-5-2010, 2010.

Durand, Y., Giraud, G., Brun, E., Merindol, L., and Martin, E.: A computer-based system simulating snowpack structures as a tool for regional avalanche forecasting, J. Glaciol., 45, 469–484, 1999.

Fierz, C., Armstrong, R., Durand, Y., Etchevers, P., Greene, E., McClung, D., Nishimura, K., Satyawali, P., and Sokratov, S.: The international classification for seasonal snow on the ground, HP-VII Technical Document in Hydrology, 83. UNESCO-IHP, Paris, France, p. 90, 2009.

Föhn, P.: The "Rutschblock" as a pratical tool for slope stability evaluation, IAHS-AISH Publ., 162, 223–228, 1987.

Gaume, J., van Herwijnen, A., Chambon, G., Wever, N., and Schweizer, J.: Snow fracture in relation to slab avalanche release: critical state for the onset of crack propagation, The Cryosphere, 11, 217–228, https://doi.org/10.5194/tc-11-217-2017, 2017.

Gerber, F., Besic, N., Sharma, V., Mott, R., Daniels, M., Gabella, M., Berne, A., Germann, U., and Lehning, M.: Spatial variability in snow precipitation and accumulation in COSMO–WRF simulations and radar estimations over complex terrain, The Cryosphere, 12, 3137–3160, https://doi.org/10.5194/tc-12-3137-2018, https://www.the-cryosphere.net/12/3137/2018/, 2018.

Giraud, G. and Navarre, J.: MEPRA et le risque de déclenchement accidentel d'avalanches, in: Les apports de la recherche scientifique à la sécurité neige, glace et avalanche. Actes de Colloque, Chamonix 30 mai-3 juin, 1995, pp. 145–150, 1995.

Grünewald, T., Schirmer, M., Mott, R., and Lehning, M.: Spatial and temporal variability of snow depth and ablation rates in a small mountain catchment, The Cryosphere, 4, 215–225, 2010.

Günther, D., Marke, T., Essery, R., and Strasser, U.: Uncertainties in Snowpack Simulations—Assessing the Impact of Model Structure, Parameter Choice, and Forcing Data Error on Point-Scale Energy Balance Snow Model Performance, Water Resources Research, 55, 2779–2800, https://doi.org/10.1029/2018WR023403, 2019.

Heck, M., van Herwijnen, A., Hammer, C., Hobiger, M., Schweizer, J., and Fäh, D.: Automatic detection of avalanches combining array classification and localization, Earth Surface Dynamics, 7, 491–503, https://doi.org/10.5194/esurf-7-491-2019, 2019.

Helbig, N. and Löwe, H.: Shortwave radiation parameterization scheme for subgrid topography, Journal of Geophysical Research: Atmospheres, 117, D03 112, https://doi.org/10.1029/2011JD016465, 2012.

Helbig, N. and van Herwijnen, A.: Subgrid parameterization for snow depth over mountainous terrain from flat field snow depth, Water Resources Research, 53, 1444–1456, https://doi.org/10.1002/2016WR019872, https://agupubs.onlinelibrary.wiley.com/doi/abs/10.1002/2016WR019872, 2017.

Helbig, N., Mott, R., van Herwijnen, A., Winstral, A., and Jonas, T.: Parameterizing surface wind speed over complex topography, Journal of Geophysical Research: Atmospheres, 122, 651–667, https://doi.org/10.1002/2016JD025593, https://agupubs.onlinelibrary.wiley.com/doi/abs/10.1002/2016JD025593, 2017.

Horton, S., Schirmer, M., and Jamieson, B.: Meteorological, elevation, and slope effects on surface hoar formation, The Cryosphere, 9, 1523–1533, https://doi.org/10.5194/tc-9-1523-2015, https://tc.copernicus.org/articles/9/1523/2015/, 2015.

Jamieson, B., Zeidler, A., and Brown, C.: Explanation and limitations of study plot stability indices for forecasting dry snow slab avalanches in surrounding terrain, Cold Regions Science and Technology, 50, 23 – 34, https://doi.org/https://doi.org/10.1016/j.coldregions.2007.02.010, http://www.sciencedirect.com/science/article/pii/S0165232X0700050X, snow and Avalanches EGU 2006, 2007.

Jamieson, B., Haegeli, P., and Schweizer, J.: Field observations for estimating the local avalanche danger in the Columbia Mountains of Canada, Cold Reg. Sci. Technol., 58, 84 – 91, https://doi.org/10.1016/j.coldregions.2009.03.005, 2009.

Jamieson, J. and Johnston, C.: Snowpack characteristics associated with avalanche accidents, Canadian Geotechnical Journal, 29, 862–866, 1992.

Jamieson, J. and Johnston, C.: Refinements to the stability index for skier-triggered dry-slab avalanches, Ann. Glaciol., 26, 296–302, https://doi.org/10.3189/1998AoG26-1-296-302, 1998.

Jamieson, J. and Johnston, C.: Evaluation of the shear frame test for weak snowpack layers, Ann. Glaciol., 32, 59–69, 2001.

Kirchner, P. B., Bales, R. C., Molotch, N. P., Flanagan, J., and Guo, Q.: LiDAR measurement of seasonal snow accumulation along an elevation gradient in the southern Sierra Nevada, California, Hydrology and Earth System Sciences, 18, 4261–4275, https://doi.org/10.5194/hess-18-4261-2014, https://www.hydrol-earth-syst-sci.net/18/4261/2014/, 2014.

Lafaysse, M., Morin, S., Coléou, C., Vernay, M., Serça, D., Besson, F., Willemet, J.-M., Giraud, G., and Durand, Y.: Towards a new chain of models for avalanche hazard forecasting in French mountain ranges, including low altitude mountains, in: Proceedings of the International Snow Science Workshop Grenoble, Chamonix Mont-Blanc, France, pp. 162–166, 2013.

Lafaysse, M., Cluzet, B., Dumont, M., Lejeune, Y., Vionnet, V., and Morin, S.: A multiphysical ensemble system of numerical snow modelling, The Cryosphere, 11, 1173–1198, 2017.

Lapo, K. E., Hinkelman, L. M., Raleigh, M. S., and Lundquist, J. D.: Impact of errors in the downwelling irradiances on simulations of snow water equivalent, snow surface temperature, and the snow energy balance, Water Resources Research, 51, 1649–1670, https://doi.org/10.1002/2014WR016259, https://agupubs.onlinelibrary.wiley.com/doi/abs/10.1002/2014WR016259, 2015.

Lehning, M., Bartelt, P., and Brown, B.: SNOWPACK model calculations for avalanche warning based upon a new network of weather and snow stations, Cold Reg. Sci. Technol., 30, 145–157, 1999.

Lehning, M., Bartelt, P., Brown, B., and Fierz, C.: A physical SNOWPACK model for the Swiss avalanche warning: Part III: meteorological forcing, thin layer formation and evaluation, Cold Reg. Sci. Technol., 35, 169 – 184, https://doi.org/10.1016/S0165-232X(02)00072-1, 2002.

Lehning, M., Fierz, C., Brown, B., and Jamieson, B.: Modeling snow instability with the snow-cover model SNOWPACK, Ann. Glaciol., 38, 331–338, https://doi.org/10.3189/172756404781815220, 2004.

Lehning, M., Völksch, I., Gustafsson, D., Nguyen, T., Stähli, M., and Zappa, M.: ALPINE3D: A detailed model of mountain surface processes and its application to snow hydrology, Hydrol. Process., 20, 2111–2128, 2006.

Liston, G. E.: Representing Subgrid Snow Cover Heterogeneities in Regional and Global Models, Journal of Climate, 17, 1381–1397, https://doi.org/10.1175/1520-0442(2004)017<1381:RSSCHI>2.0.CO;2, https://doi.org/10.1175/1520-0442(2004)017<1381:RSSCHI>2.0.CO;2, 2004.

Martin, E., Giraud, G., Lejeune, Y., and Boudart, G.: Impact of a climate change on avalanche hazard, Ann. Glaciol., 32, 163–167, https://doi.org/10.3189/172756401781819292, 2001.

McClung, D. M. and Schaerer, P.: The Avalanche Handbook, The Mountaineers, Seattle, Washington, U.S.A, 2006.

Miller, D. A. and Adams, E. E.: A microstructural dry-snow metamorphism model for kinetic crystal growth, J. Glac., 55, 1003–1011, 2009.

Monti, F., Gaume, J., Van Herwijnen, A., and Schweizer, J.: A simplified approach to assess the skier-induced stress within a multi-layered snowpack, Nat. Hazard Earth Syst. Sci. Discuss., 3, 4833–4869, 2015.

Monti, F., Gaume, J., van Herwijnen, A., and Schweizer, J.: Snow instability evaluation: calculating the skier-induced stress in a multi-layered snowpack, Natural Hazards and Earth System Sciences, 16, 775–788, https://doi.org/10.5194/nhess-16-775-2016, 2016.

Morin, S., Horton, S., Techel, F., Bavay, M., Coléou, C., Fierz, C., Gobiet, A., Hagenmuller, P., Lafaysse, M., Ližar, M., Mitterer, C., Monti, F., Müller, K., Olefs, M., Snook, J. S., van Herwijnen, A., and Vionnet, V.: Application of physical snowpack models in support of operational avalanche hazard forecasting: A status report on current implementations and prospects for the future, Cold Regions Science and Technology, 170, 102 910, https://doi.org/10.1016/j.coldregions.2019.102910, http://www.sciencedirect.com/science/article/pii/S0165232X19302071, 2020.

Mott, R. and Lehning, M.: Meteorological Modeling of Very High-Resolution Wind Fields and Snow Deposition for Mountains, Journal of Hydrometeorology, 11, 934–949, https://doi.org/10.1175/2010JHM1216.1, 2010.

Pollack, H. N., Hurter, S. J., and Johnson, J. R.: Heat flow from the Earth's interior: Analysis of the global data set, Reviews of Geophysics, 31, 267–280, https://doi.org/10.1029/93RG01249, 1993.

Raleigh, M., Lundquist, J., and Clark, M.: Exploring the impact of forcing error characteristics on physically based snow simulations within a global sensitivity analysis framework, Hydrology and Earth System Sciences, 19, 3153–3179, 2015.

Reuter, B. and Schweizer, J.: Describing snow instability by failure initiation, crack propagation, and slab tensile support, Geophysical Research Letters, 45, 7019–7027, https://doi.org/10.1029/2018GL078069, 2018.

Reuter, B., Schweizer, J., and van Herwijnen, A.: A process-based approach to estimate point snow instability, The Cryosphere, 9, 837–847, 2015.

Reuter, B., Richter, B., and Schweizer, J.: Snow instability patterns at the scale of a small basin, Journal of Geophysical Research: Earth Surface, 121, 257–282, https://doi.org/10.1002/2015JF003700, https://agupubs.onlinelibrary.wiley.com/doi/abs/10.1002/2015JF003700, 2016.

Richter, B., Schweizer, J., Rotach, M. W., and van Herwijnen, A.: Validating modeled critical crack length for crack propagation in the snow cover model SNOWPACK, The Cryosphere, 13, 3353–3366, https://doi.org/10.5194/tc-13-3353-2019, https://www.the-cryosphere.net/13/3353/2019/, 2019.

Saltelli, A. and Annoni, P.: How to avoid a perfunctory sensitivity analysis, Environmental Modelling & Software, 25, 1508–1517, 2010.

Saltelli, A., Annoni, P., Azzini, I., Campolongo, F., Ratto, M., and Tarantola, S.: Variance based sensitivity analysis of model output. Design and estimator for the total sensitivity index, Computer Physics Communications, 181, 259 – 270, https://doi.org/10.1016/j.cpc.2009.09.018, http://www.sciencedirect.com/science/article/pii/S0010465509003087, 2010.

Sauter, T. and Obleitner, F.: Assessing the uncertainty of glacier mass-balance simulations in the European Arctic based on variance decomposition, Geoscientific Model Development, 8, 3911–3928, 2015.

Scapozza, C.: Entwicklung eines dichte- und temperaturabhängigen Stoffgesetzes zur Beschreibung des visko-elastischen Verhaltens von Schnee, Ph.D. thesis, ETH Zürich, 2004.

Schlögl, S., Marty, C., Bavay, M., and Lehning, M.: Sensitivity of Alpine3D modeled snow cover to modifications in DEM resolution, station coverage and meteorological input quantities, Environmental Modelling & Software, 83, 387 – 396, https://doi.org/10.1016/j.envsoft.2016.02.017, 2016.

Schweizer, J. and Jamieson, J.: Snow cover properties for skier triggering of avalanches, Cold Reg. Sci. Technol., 33, 207–221, 2001.

Schweizer, J. and Jamieson, J.: A threshold sum approach to stability evaluation of manual snow profiles, Cold Reg. Sci. Technol., 47, 50–59, https://doi.org/10.1016/j.coldregions.2006.08.011, 2007.

Schweizer, J. and Reuter, B.: A new index combining weak layer and slab properties for snow instability prediction, Natural Hazards and Earth System Sciences, 15, 109–118, https://doi.org/10.5194/nhess-15-109-2015, https://www.nat-hazards-earth-syst-sci.net/15/109/2015/, 2015.

Schweizer, J., Jamieson, J., and Schneebeli, M.: Snow avalanche formation, Rev. Geophys., 41, 1016, https://doi.org/10.1029/2002RG000123, 2003a.

Schweizer, J., Kronholm, K., and Wiesinger, T.: Verification of regional snowpack stability and avalanche danger, Cold Reg. Sci. Technol., 37, 277–288, 2003b.

Schweizer, J., Bellaire, S., Fierz, C., Lehning, M., and Pielmeier, C.: Evaluating and improving the stability predictions of the snow cover model SNOWPACK, Cold Reg. Sci. Technol., 46, 52–59, 2006.

Schweizer, J., Reuter, B., van Herwijnen, A., Richter, B., and Gaume, J.: Temporal evolution of crack propagation propensity in snow in relation to slab and weak layer properties, The Cryosphere, 10, 2637–2653, https://doi.org/10.5194/tc-10-2637-2016, 2016.

Slaughter, A. E.: Numerical analysis of conditions necessary for near-surface snow metamorphism, PhD thesis, Montana State University, Bozeman, Montana, USA, https://search.proquest.com/openview/4e7f8f2f70589efc81d6d9198d67ee62/1?pq-origsite=gscholarcbl=18750diss=y, 2010.

Sobol', I. M.: On sensitivity estimation for nonlinear mathematical models, Matematicheskoe modelirovanie, 2, 112–118, 1990.

Staron, P. J., Adams, E. E., and Miller, D. A.: Formation of Depth Hoar Resulting from Thermal Optimization of Snow Microstructure, Proceedings of International Snow Science Workshop, Anchorage, USA, pp. 186–193, 2012.

Stössel, F., Guala, M., Fierz, C., Manes, C., and Lehning, M.: Micrometeorological and morphological observations of surface hoar dynamics on a mountain snow cover, Water Resources Research, 46, W04 511, https://doi.org/10.1029/2009WR008198, https://agupubs.onlinelibrary.wiley.com/doi/abs/10.1029/2009WR008198, 2010.

van Herwijnen, A. and Jamieson, B.: Snowpack properties associated with fracture initiation and propagation resulting in skier-triggered dry snow slab avalanches, Cold Reg. Sci. Technol., 50, 13–22, https://doi.org/10.1016/j.coldregions.2007.02.004, 2007.

van Herwijnen, A., Gaume, J., Bair, E. H., Reuter, B., Birkeland, K. W., and Schweizer, J.: Estimating the effective elastic modulus and specific fracture energy of snowpack layers from field experiments, J. Glaciol., 62, 997–1007, https://doi.org/10.1017/jog.2016.90, 2016.

Vernay, M., Lafaysse, M., Mérindol, L., Giraud, G., and Morin, S.: Ensemble forecasting of snowpack conditions and avalanche hazard, Cold Reg. Sci. Technol., 120, 251 – 262, https://doi.org/10.1016/j.coldregions.2015.04.010, 2015.

Vionnet, V., Brun, E., Morin, S., Boone, A., Martin, E., Faroux, S., Moigne, P. L., and Willemet, J.-M.: The detailed snowpack scheme Crocus and its implementation in SURFEX v7.2, Geosci. Model. Dev., 5, 773–791, https://doi.org/10.5194/gmd-5-773-2012, 2012.

Vionnet, V., Martin, E., Masson, V., Guyomarc'H, G., Naaim Bouvet, F., Prokop, A., Durand, Y., and Lac, C.: Simulation of wind-induced snow transport and sublimation in alpine terrain using a fully coupled snowpack/atmosphere model, The Cryosphere, 8, p. 395 – p. 415, https://doi.org/10.5194/tc-8-395-2014, https://hal.archives-ouvertes.fr/hal-00979646, 2014.

Vögeli, C., Lehning, M., Wever, N., and Bavay, M.: Scaling Precipitation Input to Spatially Distributed Hydrological Models by Measured Snow Distribution, Frontiers in Earth Science, 4, 108, https://doi.org/10.3389/feart.2016.00108, https://www.frontiersin.org/article/10.3389/feart.2016.00108, 2016.

Wever, N., Schmid, L., Heilig, A., Eisen, O., Fierz, C., and Lehning, M.: Verification of the multi-layer SNOWPACK model with different water transport schemes, The Cryosphere, 9, 2271–2293, 2015.

Winstral, A., Elder, K., and Davis, R. E.: Spatial Snow Modeling of Wind-Redistributed Snow Using Terrain-Based Parameters, Journal of Hydrometeorology, 3, 524–538, https://doi.org/10.1175/1525-7541(2002)003<0524:SSMOWR>2.0.CO;2, 2002.

WSL Institute for Snow and Avalanche Research SLF: WFJ_MOD: Meteorological and snowpack measurements from Weissfluhjoch, WSL Institute for Snow and Avalanche Research SLF, https://doi.org/10.16904/1, 2015.